European Journal of Medicinal Chemistry 208 (2020) 112833

Contents lists available at ScienceDirect

European Journal of Medicinal Chemistry

journal homepage: http://www.elsevier.com/locate/ejmech

Research paper

Discovery of novel VX-809 hybrid derivatives as F508del-CFTR correctors by molecular modeling, chemical synthesis and biological assays

Alice Parodi [a, 1], Giada Righetti [b, 1], Emanuela Pesce [c], Annalisa Salis [d], Bruno Tasso [b], Chiara Urbinati [e], Valeria Tomati [c], Gianluca Damonte [a, d], Marco Rusnati [e], Nicoletta Pedemonte [c], Elena Cichero [d, **], Enrico Millo [a, d, *]

[a] Department of Experimental Medicine, Section of Biochemistry, University of Genoa, Viale Benedetto XV 1, 16132, Genoa, Italy
[b] Department of Pharmacy, Section of Medicinal Chemistry, School of Medical and Pharmaceutical Sciences, University of Genoa, Viale Benedetto XV, 3, 16132, Genoa, Italy
[c] UOC Genetica Medica, IRCCS Istituto Giannina Gaslini, Genova, Italy
[d] Center of Excellence for Biomedical Research (CEBR), University of Genoa, Viale Benedetto XV 9, 16132, Genoa, Italy
[e] Department of Molecular and Translational Medicine, University of Brescia, 25123, Brescia, Italy

ARTICLE INFO

Article history:
Received 16 June 2020
Received in revised form
4 September 2020
Accepted 5 September 2020
Available online 12 September 2020

Keywords:
Cystic fibrosis
F508del-CFTR
CFTR Corrector
Aminoarylthiazole
Docking
Surface plasmon resonance

ABSTRACT

Cystic fibrosis (CF) is the autosomal recessive disorder most recurrent in Caucasian populations. It is caused by different mutations in the cystic fibrosis transmembrane regulator protein (CFTR) gene, with F508del being the most common. During the last years, small-molecule therapy chosen to contrast CF relied on compounds that correct CFTR misfolding and ER retention (correctors such as VX-809), or defective channel gating (potentiators such as VX-770). Combination therapy with the two series of drugs has been applied, leading to the approval of several multi-drugs such as Orkambi.

Despite this, this treatment proved to be only partially effective making the search for novel modulators an urgent need to contrast CF. Recently, we reported compound **2a** as reference compound of a series of aminoarylthiazole-VX-809 hybrid derivatives exhibiting promising F508del-CFTR corrector ability. Herein, we report exploring the docking mode of the prototype VX-809 and of **2a** in order to derive useful guidelines for the rational design of novel optimized analogues. To demonstrate experimentally their effective F508del-CFTR-binding and rescuing potential, the most promising derivatives had been synthesized and evaluated in biological assays including YFP functional assay on F508del-CFTR CFBE41o-cells, trans epithelial electrical resistance (TEER) and surface plasmon resonance (SPR). This multidisciplinary strategy led to the discovery of a second series of hybrids including **7j** and **7m** endowed with higher potency than the prototype.

1. Introduction

Cystic Fibrosis (CF) is a lethal monogenic disease caused by inherited mutations in a gene that encodes the CF transmembrane conductance regulator (CFTR) protein, an ATP-binding cassette (ABC) transporter that functions as a Cl^- channel with complex

Abbreviations: CF, cystic fibrosis; CFTR, Cystic Fibrosis transmembrane conductance regulator protein; AAT, aminoarylthiazole; DMAP, 4-(*N*,*N*-dimethylamino)pyridine; DIPEA, *N*,*N*-Diisopropylethylamine; HATU, Hexafluorophosphate azabenzotriazole tetramethyl uronium; BOC_2O, di-*tert*-butyl carbonate; HPLC, high performance liquid chromatography; ESI-MS, electrospray mass spectrometry; HS-YFP, halide-sensitive yellow fluorescent protein; TEER/PD, *Trans*-epithelial electrical resistance and potential difference measurements; SPR, Surface Plasmon Resonance.

* Corresponding author. Department of Experimental Medicine, Section of Biochemistry, University of Genoa, Viale Benedetto XV 1, 16132, Genoa, Italy.
** Corresponding author. Department of Pharmacy, Section of Medicinal Chemistry, School of Medical and Pharmaceutical Sciences, University of Genoa, Viale Benedetto XV, 3, 16132, Genoa, Italy.
E-mail addresses: cichero@difar.unige.it (E. Cichero), enrico.millo@unige.it (E. Millo).
[1] These authors contributed equally to this work.

https://doi.org/10.1016/j.ejmech.2020.112833
0223-5234/

regulation [1]. These mutations cause improper localization and functioning of this chloride channel in lung, pancreas, and intestine thus affecting the normal fluid homeostasis [1]. In CF the lungs are the most affected organ due to the accumulation of thick mucus, which results into bacterial load and associated chronic inflammation [2].

More than 2000 mutations have been identified in the CFTR gene, most of them being very rare, although a pathogenic effect has been demonstrated only for about 350 variants. By far the most common disease-causing mutation is F508del, the deletion of the phenylalanine residue at position 508 of the CFTR amino acid sequence [3].

Although F508del affects only one residue located on the surface of the first nucleotide-binding domain (NBD1) [4], structural studies reveal that the absence of this crucial amino acid could cause structural changes to the ABC-alpha subdomain of NBD1 [5]. Indeed, loss of Phe-508 breaks up domain-domain interactions critical for correct assembly and function of CFTR [6–11]. F508del-CFTR is recognized as abnormal by the endoplasmic reticulum quality control machinery, leading to degradation by the proteasome [12,13]. Thus, F508del mutation principally disrupts the processing and intracellular transport of CFTR protein. Nevertheless, any F508del-CFTR that escapes to the plasma membrane can present two further problems: reduced stability [14] and altered channel gating [15]. As a consequence, novel state-of-the-art therapies are needed to address all these problems.

To overtake the defective expression and function of CF mutants, administering CFTR modulators has been applied. In detail, a CFTR modulator is a pharmaceutical agent that targets a specific defect in the CFTR protein. This modulator does not correct mutations in the gene but rather acts to solve the errors that occur post transcriptionally, either during protein folding, trafficking up to the plasma membrane, or CFTR functioning. The CFTR modulators can be classified in different classes following their different mechanisms of action.

In particular, two classes of small molecules have been developed named CFTR correctors and CFTR potentiators [12].

CFTR correctors (eg Lumacaftor; VX-809) [16] allow the mutant proteins to traffic to the plasma membrane while CFTR potentiators (e.g. Ivacaftor; VX-770) [17] strongly increase channel gating. Since neither Lumacaftor nor Ivacaftor, by themselves, seem to have clinical benefit for CF patients with the F508del mutation [18,19], combination therapy with the two drugs has been applied. This improved lung function and disease stability [20], leading to the approval of lumacaftor-ivacaftor combination therapy (named Orkambi). Dual-combination therapies such as Orkambi and Symdeko (containing the corrector Tezacaftor, i.e. VX-661, an analogue of VX-809, together with Ivacaftor) have been approved for healing lung function to a modest degree in F508del homozygous patients [21]. Triple combinations using two distinct correctors and a potentiator showed good clinical benefit in patients with a F508del-CFTR mutation on at least one allele [22–24]. However, the effectiveness of these combinations through the multitude of genotypes remains to be evaluated.

In the search for new drugs for CF treatment, in our previous works we reported the rational design, chemical synthesis and biochemical characterization of a novel library of aminoarylthiazole (AAT) and VX-809 hybrid derivatives, exhibiting interesting properties as F508del-CFTR correctors [25].

This kind of substitution proved also to be effective as shown by other analogues of VX-809 reported in the literature, such as the two highly related congeners ALK-809 and SUL-809 featuring an amide and an acylsulfonamide function instead of the carboxylic moiety of the prototype (Fig. 1) [26], VX-661 (Tezacaftor), successfully evaluated on patients in combination with VX-770 [27], or a library of compounds synthesized coupling 1-(2,2-difluorobenzo [d] [1,3]-dioxol-5-yl)cyclopropanecarboxylic acid with various amine monomers, as described by Wang et al. [28].

Maintaining the benzodioxole group appears a recurrent strategy also taking into account the results obtained with GLPG-2222 [28] and with other correctors described by AbbVie and Galapagos companies, in which this effective substituent was tethered to the chroman ring or to the tetrahydropyran ring [29].

Our in-house set of compounds has been defined “hybrid compounds” since their structures were really thought of as a hybrid between the AAT and the VX-809 scaffolds. Among them, we identified a number of analogues featuring EC_{50} values in terms of CFTR rescue ability comprised between 0.09 and 0.2 μM, with compound **2a** being the most active ($EC_{50} = 0.087$ μM) (Fig. 1) [25].

On this basis, herein we discuss the design and discovery of a new library of optimized hybrids, displaying ameliorated potency values (EC_{50} values spanning from 0.02 to 0.1 μM), which have been obtained by modifying some groups on the main core of the compounds.

In particular, we proceeded with molecular docking studies focused on the previously identified hybrid prototype **2a**, in order to gain more information about the putative binding mode of the corrector to the CFTR NBD1 domain. This allowed us to better explore the structure-activity relationship (SAR) within the hybrid series and to point out novel beneficial chemical substitutions to decorate the thiazole ring. In addition, the selection of the most promising compounds to be synthesized has been performed also taking into account the information and mathematical prediction of the QSAR model we previously built and published [25].

The following synthetic efforts, combined with the biochemical evaluation of the compounds as effective F508del-CFTR binders through surface plasmon resonance (SPR) and their subsequent biological evaluation as F508del-CFTR correctors, validated the effectiveness of the hybrid core in the search for novel potent CFTR modulators. The overall results have provided novel SAR information on hybrids as correctors and led to the identification of molecules with a particular ability to rescue F508del-CFTR.

2. Results and discussion

2.1. Rational design of novel hybrids as F508del-CFTR correctors

In our previous work, we reported QSAR analyses on different series of correctors reported in the literature [25]. This allowed us to identify eight descriptors explaining the corrector ability range of the library, being five of them bi- and three-dimensional descriptors (2D and 3D). These included parameters related to atoms and bound counts (b_single, a_IC and a_nH) and surface area descriptors (Vsurf_DD12 and Vsurf_W8). The connectivity-based descriptor chi1, the so-called distance matrix parameter weinerPol and the potential energy descriptor E_nb were also retained [25].

As we discussed, these promoted the design of branched scaffolds enriched with flexible substituents and quite polar moieties within overall limited and bulky conformations. Accordingly, we designed and synthesized a number of hybrids endowed with a promising CFTR rescue ability, with **2a** being the most potent.

Beyond QSAR prediction, herein we proceeded with preliminary docking studies in order to gain further useful information to guide the rational design of new **2a** analogues. These calculations have been performed taking into account the theoretical studies so far disclosed in the literature concerning the reference corrector VX-809. Indeed, a number of in silico studies deeply investigated the putative binding mode of VX-809 to different portions of the CFTR protein, providing support to multiple sites involved in the

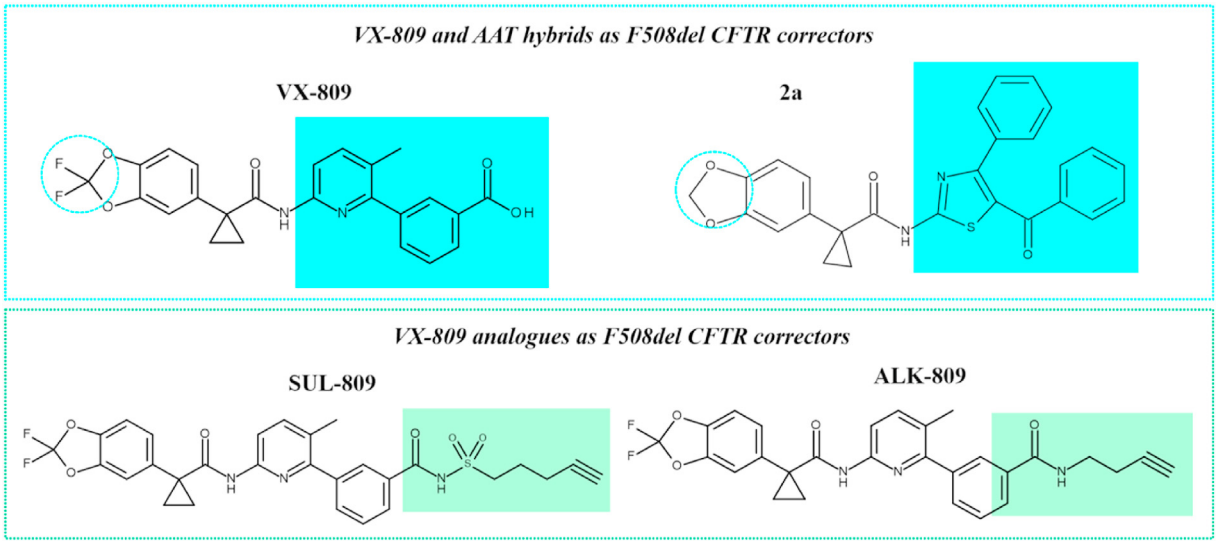

Fig. 1. Chemical structure of VX-809, ALK-809, SUL-809 and of the hybrid **2a**. The structural variation experienced by **2a** and by ALK-809, SUL-809 with respect to the prototype VX-809 are highlighted in cyan and green, respectively. (For interpretation of the references to color in this figure legend, the reader is referred to the Web version of this article.)

corrector mechanism of action [30].

Accordingly, while data reported in the literature surmised VX-809 directly targeting the full-length F508del-CFTR protein, with a possible binding site at the NBD1-ICL4 interface [31], other findings suggested that VX-809 may stabilize an *N*-terminal domain in CFTR that contains membrane-spanning domain 1 [32].

On this basis, several virtual screening approaches moved the discovery of novel F508del correctors exploring the NBD1:NBD2 interface so as the MSD: NBD1, supporting a fundamental role played by NBD1 at the corrector binding site [33].

In this context, our research group recently reported surface plasmon resonance (SPR) studies on F508del-NBD1 performed with the corrector VX-809 and molecular docking and dynamics simulations, highlighting a statistically significant correlation between the observed binding capability to F508del-NBD1 and the results of the computational methods. On the whole, these results demonstrated a strong agreement between the theoretical prediction and the experimental SPR-based data, supporting a key role played at the NBD1 level of CFTR by the corrector VX-809 to exert any CFTR rescue ability [34].

Thus, in order to better investigate the putative mechanism of action of this corrector at the biological target, we applied molecular docking studies around the human F508del-CFTR NBD1 domain, taking VX-809 and two analogues ALK-809 and SUL-809 as reference compounds (as scoring parameters, the predicted energy values of the NBD1-corrector complexes were listed in Supporting **information S1**) [26]. In particular, these two congeners are characterized by an amide and a sulfonamide function instead of the carboxylic moiety of the prototype, lacking the possibility to exhibit a negatively charged group.

Based on docking calculations, two putative binding positioning for the corrector VX-809, namely POS1 and POS2, can be described. As shown in Fig. 2A (POS1), the oxygen atom of the carboxamide group of VX-809 is involved in one H-bond with the N659 side-chain, while the carboxylic group is engaged in ionic contacts with K464 and H-bonds with T460 and G461. The aromatic rings of the corrector occupy the protein pocket delimited by S573, G576, V603 and A655, exhibiting van der Waals contacts while the benzodioxole core is projected towards Y577 and E656.

Concerning POS2 (Fig. 2B), two H-bonds with the key residues K464 and T465 are formed by the two oxygen atoms of the benzodioxole core. The negatively-charged carboxylic group of the corrector is H-bonded to the backbone of E656. The overall positioning recognized as POS2 allowed VX-809 to occupy the same binding pocket described for POS1, since the aromatic rings and all the substituents are placed in proximity to the previously cited G461, V603, A655 and N659.

Conversely, docking calculations performed on ALK-809 and SUL-809 revealed a unique putative binding mode in agreement with the previously named POS2 of VX-809. As shown in Fig. 3, both compounds display one H-bond between the (sulfon)amide moiety and the backbone of E656 while the oxygen atoms of the benzodioxole ring feature polar contacts with K464 and T465. Finally, the amide group linked at the main core of the correctors is projected towards N659 with H-bonds. Since VX-809 as well as the two analogues ALK-809 and SUL-809 exhibit comparable potency as CFTR correctors, it could be inferred that POS2 represents the bioactive conformation of VX-809 analogues.

Docking calculations performed around our first series of hybrids proved to be in agreement with POS2 proposed for the aforementioned VX-809 analogues and also allowed us to better explain the SAR within this series of promising correctors.

As shown in Supporting **information S2** for 5-unsubstituted AATs, the introduction of a *p*-substituted phenyl ring linked at position 4 of the main thiazole was preferred leading to compounds featuring higher potency values than those of the *m*-substituted analogues.

Conversely, an opposite trend can be observed when a methyl group or ester moiety decorates position 5 of the AAT, making the *m*-substitution more effective. In addition, a perspective of all the results underlines a comparable behavior exhibited by those compounds showing the benzodioxole ring instead of the fluorinate analogue, and a beneficial role played by concomitant substitutions at positions 4 and 5 of the thiazole main core [25]. In particular, derivatives **2a**-**2c** displayed higher potency values within this series of correctors, with **2b**-**2c** being characterized by an ester moiety linked to position 5 of the thiazole. The most active analogue **2a** displayed a benzoyl group at the same position.

Docking calculations of these compounds revealed that for all of them the carboxamide moiety is involved in one H-bond with N659, while the two oxygen atoms of the benzodioxole ring were H-bonded to K464 and T465. In the case of **2b** (EC_{50} = 0.30 μM) and

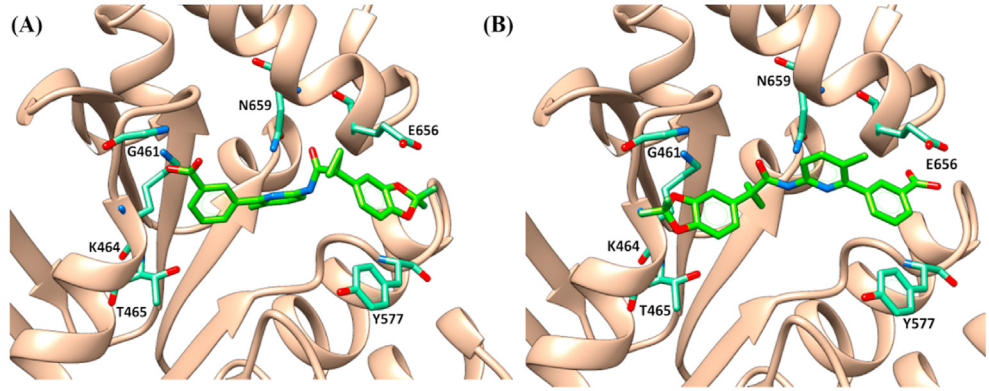

Fig. 2. Selected docking poses of VX-809 within the CFTR hNBD1 domain as POS1 (A) and POS2 (B). The most important residues are labelled.

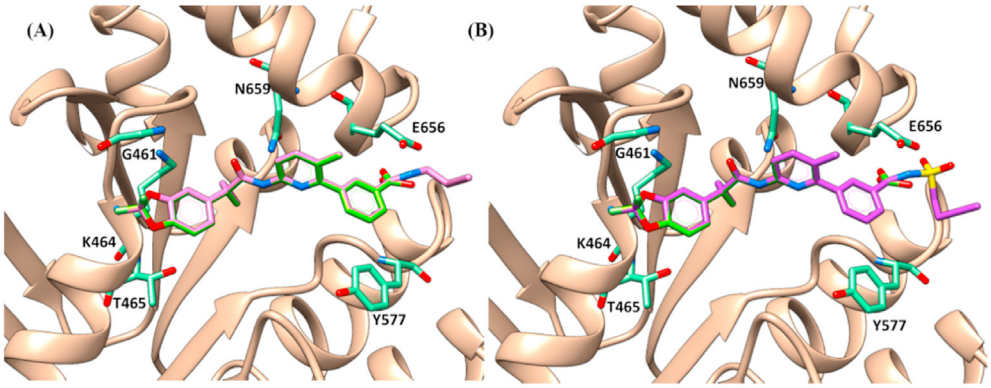

Fig. 3. Selected docking poses of ALK-809 (*C* atom; pink) (A) and SUL-809 (*C* atom; purple) (B) within the CFTR hNBD1 domain, both in agreement both POS2 of VX-809 (*C* atom; green). The most important residues are labelled. (For interpretation of the references to color in this figure legend, the reader is referred to the Web version of this article.)

2c (EC_{50} = 0.55 μM), the presence of the quite flexible ester group at position 5 of the thiazole guides the positioning of the compounds based on the concomitant *m*- or *p*-substituted phenyl ring tethered to position 4 of the AAT with H-bonding of the hydroxyl group of the Y577 sidechain or the E656 backbone (Supporting **information S3**) via the oxygen atom of the carbonyl group.

However, based on the promising potency of both correctors, it is thought that H-bonding to N659, K464 and T465 represents a key requirement of correctors, while interacting with E656 or Y577 could efficiently stabilize the modulator within the hNBD1 domain.

The most probable docking mode of **2a** (EC_{50} = 0.087 μM) proved to be in agreement with those of VX-809 (POS2) and SUL-809, as shown in Fig. 4.

The carboxamide moiety and the benzodioxole ring of the hybrid highly simulate the binding mode proposed for the prototype VX-809 and for the related congener SUL-809, showing the same contacts. On the whole, the thiazole ring proved to be a good bioisoster of the pyridine one maintaining the previously mentioned interactions with the biological target.

Notably, hydrophobic interactions displayed by the benzoic group of VX-809 and by the sulfonamide moiety of SUL-809 are experienced by the two aromatic rings connected to the **2a** thiazole core while the oxygen atom of the benzoyl group interacts with the E656 side-chain, as reported for the two reference compounds.

This information opened the possibility to explore the role played by different substitutions on the benzoyl moiety of **2a** in order to clarify the relevance of hydrophobic and polar contacts especially with Y577, and the possibility of modifying the carbonyl function with other H-bond acceptor moieties properly tethered to the thiazole core. In addition, structural variations involving the substituent linked to position 4 of the thiazole ring could be managed in an attempt to mimic the methyl group of corrector VX-809.

Herein we report the chemical synthesis and biological evaluation of **2a** analogues focusing on variations of the benzoyl core (compounds **7a-7z, 12a-12d, 24a-24c**), whose potency profile in terms of CFTR rescue ability have been predicted by means of the QSAR model we previously built prior to synthesis **(**Supporting **information S4).**

2.2. Chemistry

To synthesize all the compounds we applied a known synthetic route with appropriate modifications [25]. To obtain the benzodioxole substituted portion we use the well-known cyclopropanation of active methylene compounds as previously published [25].

The substituted aminoarylthiazoles are synthesized in different ways depending of the substituents at position 5 of the thiazole ring.

For the general structures of (2-amino-4-arylthiazol-5-yl) (aryl) methanone derivatives a convergent synthesis was developed (Scheme 1) in accord with the Wang protocol with minor modifications [35]. To obtain a selective introduction of the substituent groups on the thiazole ring a protected carbamothioyl amide was conjugated with substituted α-bromoketone. A mixture of 1-[4-(methoxy)phenyl]methanamine **1** and 4-(methoxy)benzaldehyde **2** was heated in refluxing methanol to obtain bis((4-(methoxy)

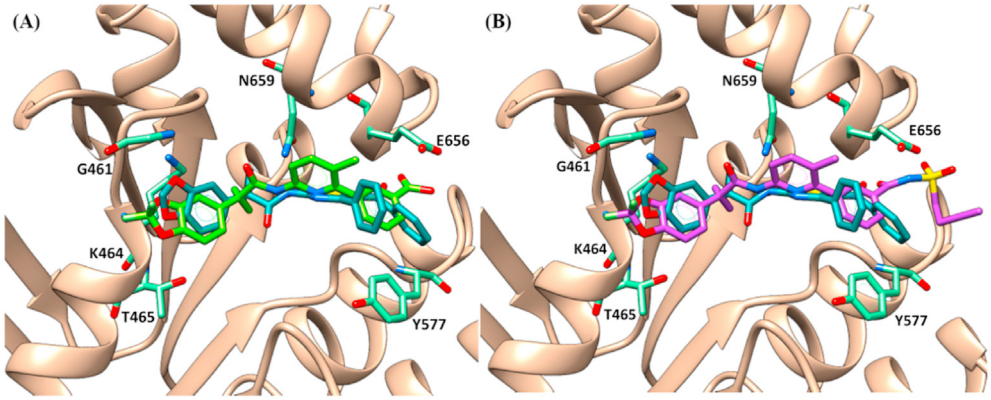

Fig. 4. Docking mode of **2a** (*C* atom; blue) in comparison with that of VX-809 (*C* atom; light green) (A) and of SUL-809 (*C* atom; purple) (B) at the hNBD1 domain of the F508del-CFTR mutant. (For interpretation of the references to color in this figure legend, the reader is referred to the Web version of this article.)

phenyl)methyl)amine **3**.

Protected carbamothioyl amide **4** was then obtained by condensation of benzoylisothiocyanate and bis ((4-(methoxy) phenyl) methyl) amine **3** in high yield.

Condensation of protected carbamothioyl amide and α-halo ketone followed by deprotection, afforded the thiazolic derivatives **5**, which were then further condensed with 1-(benzo[d] [1,3] dioxol-5-yl)cyclopropanecarboxylic acid **6** to produce the desired analogues **7a-7z**.

This last synthetic step was achieved by reaction of 2-amino-thiazole with the carboxylic group of cyclopropane carboxylic acid derivatives with uronium salt activation in anhydrous solvents [25].

For compound **12a** a different route was applied (Scheme 2). Starting from ethyl 2-amino-4-arylthiazole-5-carboxylate **8,** t-Boc protection at the aminic group was conducted to minimize decarboxylation of the thiazole ring. The protection with t-Boc also provided a high solubility of the molecule in organic solvents, allowing for high reactivity of the carboxyl group.

To prepare the carboxamide derivative **10** the appropriate 2-amino-thiazole-5-carboxylate **8** was treated with di-*tert*-butyl carbonate in the presence of 4-(*N*,*N*-dimethylamino)pyridine in tetrahydrofuran to form the corresponding *tert*-butyl carbamate that upon basic hydrolysis afforded the acid **9**. Conversion of the carboxylic acid to its uronium salt using standard peptide coupling conditions and its subsequent treatment with aniline, in the presence of diisopropylethylamine *in N, N*-DMF afforded the anilide derivative **10**, which, on further deprotection of the BOC-protecting group in trifluoroacetic acid afforded the aminothiazole **11**.

The final compound **12a** was then obtained by condensation with the carboxylic group of cyclopropanecarboxylic acid derivative **6** as previously described.

To prepare **12b** a different approach was used. *N*-(2-amino-4-(4-methoxyphenyl)thiazol-5-yl)benzamide was prepared through a two-step synthesis starting from alfa-aminoacetophenone derivative 14 (Scheme 3). The starting reagent was prepared from 4-methoxyphenacyl bromide **13** following Delepine reaction (hexamethylenetetramine in diethyl ether) as 4-methoxybenzoylmethylammonium chloride salt. Acylation of the amino functionality with benzoyl chloride proceeded efficiently to provide *N*-(2-(4-methoxyphenyl)-2-oxoethyl)benzamide **15**. Its bromination and treatment with the thiourea, following the general Hantzsch cyclocondensation pattern, was tried but without success. The very low yield of this procedure is due to the difficulty of selectively monobromination of derivative **15** as well as isolating the respective unstable intermediate *N*-(1-bromo-2-(4-methoxyphenyl)-2-oxoethyl)benzamide.

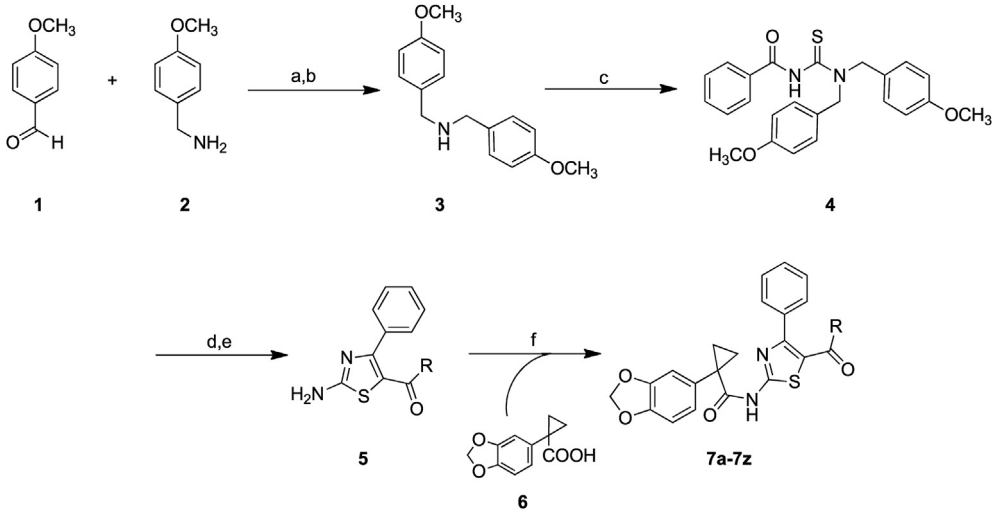

Scheme 1. Reagents and conditions: (a) methanol, reflux, 3 h; (b) $NaBH_4$, 0 °C to rt, 10 h; (c) Benzoylisothiocyanate, acetone, 0 °C, 1 h; (d) $RCOCH_2Br$, *N,N*-DMF, 85 °C, 3 h; (e) TFA, 80 °C, 36 h; (f) HATU, DIPEA, *N,N*-DMF, 50 °C, 18–24 h. For R and complete structures see Table 2.

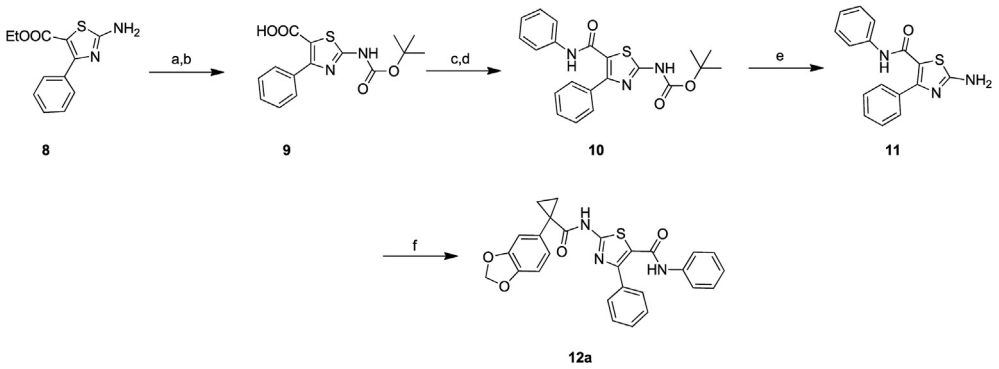

Scheme 2. Reagents and conditions: (a) BOC_2O, DMAP, THF, rt, 4 h; (b) KOH 6 N, THF:EtOH = 1:1.5, 55 °C, 4 h; (c) HATU, DIPEA, *N,N*-DMF, rt, 5 min; (d) $PhNH_2$, 40 °C, 2 h; (e) TFA:DCM = 1:1, 0 °C, 4 h; (f) **6**, HATU, DIPEA, *N,N*-DMF, 50 °C, 24 h.

There was a significant increase in yield with the one pot condensation of *N*-(2-(4-methoxyphenyl)-2-oxoethyl)benzamide with thiourea and iodine using triethylamine as catalyst under mild conditions as reported in the literature [36].

The synthesis of amide derivatives of 2-aminothiazole was achieved by condensation reaction of the 2-amino-thiazole with the carboxylic group of cyclopropanecarboxylic acid derivative **6** as previously described.

For the synthesis of the compounds **12c** and **12d,** our synthetic strategy hinged on a reaction between a substituted thiazole in position 5 and cyclopropanecarboxylic acid derivative. The functionalized thiazoles used for the substitution step were obtained as shown in Scheme 4 via adaption of reported thiazole synthesis [37]. Thiourea **17** was quantitatively activated as bis-thiazadiene **18** with excess of commercially available *N,N*-dimethylformamide dimethylacetal in methanol. The thiazole ring was formed after addition of the corresponding alfa-bromoketones **19a** and **19b** in THF. Intermediates **20a-20b**, which were not isolated, were deprotonated in situ by addition of triethylamine. The second imine, used here as a protecting group, was subsequently removed in situ with methylamine in water to form the expected products **21a** and **21b** in good yield.

The final products **12c** and **12d** were obtained by condensation of the 2-amino-thiazole with the carboxylic group of cyclopropanecarboxylic acid derivatives as previously described.

To synthesize derivatives **24a, 24b** and **24c** we applied the same synthetic route used in Scheme 1 but starting from aliphatic, heteroaromatic and heterocycle haloketones **22a, 22b** and **22c** (Scheme 5).

2.3. Effect of compounds as correctors of F508del-CFTR trafficking defect

Our goal was to identify and characterize potent and selective correctors of F508del-CFTR trafficking defect.

To verify our considerations all designed compounds were then synthesized and tested to investigate the structure-activity relationships as correctors of F508del-CFTR (Tables 1–3).

By using the YFP functional assay on F508del-CFTR CFBE41o- cells, we tested the compounds after 24 h incubation at different concentrations to extrapolate the EC_{50} values of the compounds as correctors of mutant CFTR (Tables 1–3). Activity, after incubation with these hybrids, of F508del-CFTR in the plasma membrane was determined by measuring the rate of HS-YFP quenching caused by iodide influx as previously published [25]. Activity was then compared to that of cells treated with vehicle alone (DMSO) or with the known corrector VX-809 (1 μM).

Based on our previous study [25], in which we had modified the thiazolic ring at different positions, we have identified that the most active compound **2a** (EC_{50} = 0.087 μM) was characterized by a substitution at position 5 of the thiazole ring with benzoyl group and phenyl ring linked at the thiazole position 4 (Fig. 1).

In addition, we have already demonstrated that substitution at position 5 of the thiazole ring was necessary for a good activity since the most active derivatives of the previous series all contained a substituent at position 5.

In fact, the presence of a bulky substituent (benzoyl or ethyl acetate) at C-5 might be useful in terms of improving some pharmacokinetic characteristics, while the derivatives that contain no substitution led to a decrease in corrector activity [25].

First, removal of the keto group present in the hit compound or the substitution with the amidic one led to a weak decrease in activity with respect to the benzoyl analogues: compare **12a** (EC_{50} = 1.26 μM) and **12b** (EC_{50} = 1.76 μM) vs. **2a** (Table 1).

Furthermore, we have demonstrated that the C-4 aryl group of the 2-aminothiazole is crucial for activity, as its removal [**12c** (EC_{50} = 2.57 μM) and **12d** (EC_{50} = 9.3 μM)] led to decreasing activity with respect to the progenitor (EC_{50} = 0.087 μM) (see Table 1).

Thus, we chose to initially build a series of substituted analogues Table 2, keeping intact, for comparative purpose, the phenyl ring at position 4.

First, we investigated substitutions of the phenyl ring at position 5 starting from the *para* position.

A number of different electron-withdrawing groups were

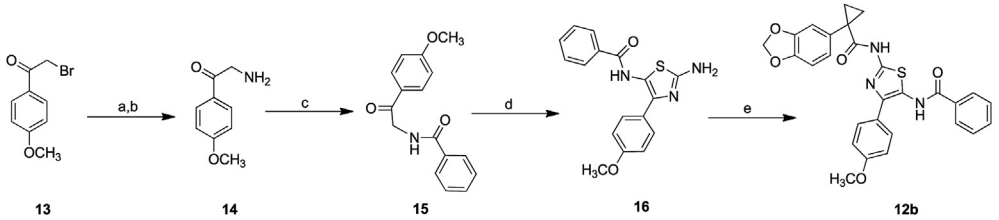

Scheme 3. Reagents and conditions: (a) hexamethylenetetramine, diethyl ether, rt, 2 h; (b) HCl conc, EtOH, reflux, 3 h; (c) C_6H_5COCl, $NaHCO_3$, THF, rt, 3 h; (d) thiourea, I_2, EtOH, TEA, 80 °C, overnight; (e) **6**, HATU, DIPEA, *N,N*-DMF, 50 °C, 24 h.

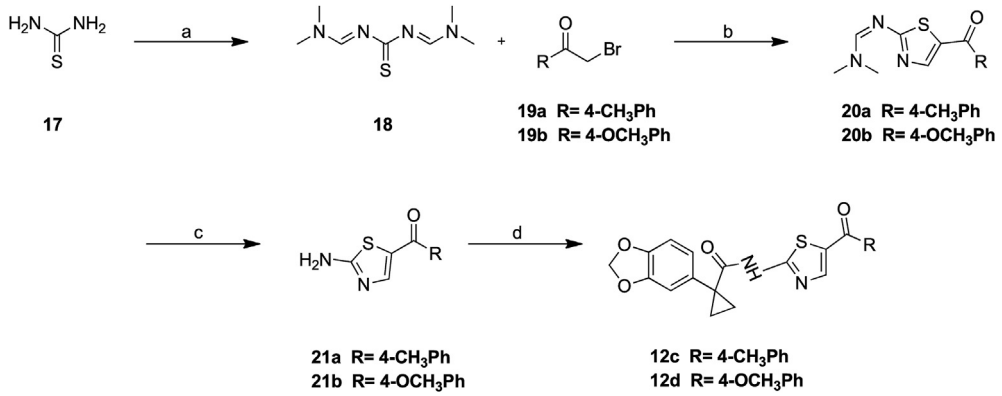

Scheme 4. Reagents and conditions: (a) *N,N*-Dimethyl formamide dimethyl acetal, DCM, reflux, 4 h; (b) THF, TEA, rt to reflux, 18 h for **20a**, 20 h for **20b**; (c) 33% aq CH_3NH_2, THF, rt, 24 h; (d) HATU, DIPEA, *N,N*-DMF, 50 °C, 24 h for **12c**, 36 h for **12d.**

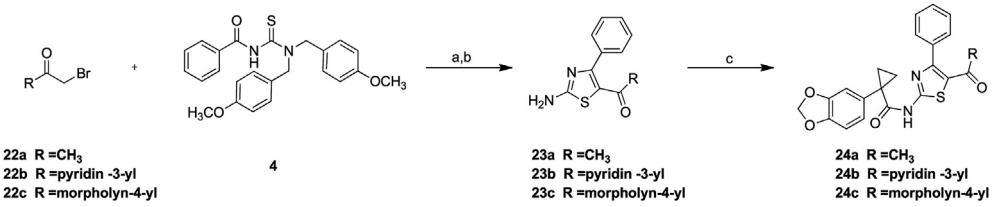

Scheme 5. Reagents and conditions: (a) *N,N*-DMF, 85 °C, 2 h; (b) TFA, 80 °C, 36 h; (c) **6**, HATU, DIPEA, *N,N*-DMF, 50 °C, 18 h for **24a**, 24 h for **24b** and **24c**.

Table 1
Chemical structure and potency profile of the novel hybrids **12a**-**12d** as F508del CFTR correctors.

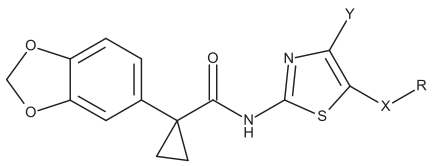

Compound	X	R	Y	EC_{50} (μM)
12a	CONH	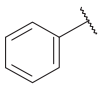	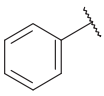	1.26
12b	NHCO	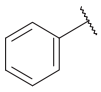	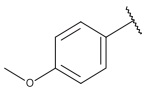	1.76
12c	CO	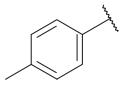	-H	2.57
12d	CO	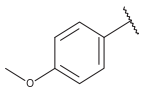	-H	9.30

anchored at this position such as a methylthio group **7a** (EC_{50} = 0.10 μM) or bromine **7b** (EC_{50} = 0.53 μM) but only the first was well tolerated and represents one of the most promising hybrids of this series. The same considerations can be made with three different compounds containing ester, carboxylic or amidic groups. In particular, only the ethyl ester derivative maintains a certain activity **7c** (EC_{50} = 0.41 μM) while the carboxylic **7d** caused a decrease in activity (EC_{50} = 7.31 μM). The amidic group, as in compound **7e,** is really deleterious for activity.

To understand if the *para* position is important for F508del-CFTR rescue, we introduced electron-donating groups in the same position. Incorporation of alkyl amino as in **7f** (EC_{50} = 0.45 μM), alkyl as in **7g** (EC_{50} = 0.43 μM) were not seen to improve the activity; so we chose to insert a methoxy group like in **7h** but no increase of activity was observed (EC_{50} = 0.45 μM). A similar result was obtained with a trifluoromethoxy group **7i** (EC_{50} = 0.36 μM). We tried to increase the hydrophobic portion of the substituent modifying the length of the alkyl chain like in derivative **7j.** Surprisingly the substitution of methyl group with a propyl one ameliorates the activity by about five times (EC_{50} = 0.017 μM). Curiously, changing the position of propoxy group from *para* to *meta* **7k** caused a reduction of activity (EC_{50} = 0.017 μM vs EC_{50} = 0.165 μM in Table 2). This characteristic could reveal a striking preference for hydrophobic groups so we decide to deepen this aspect using steric hindrance in the structure.

Three different compounds were designed and built with a second aromatic ring like thiophene for **7l** (EC_{50} = 1.06 μM) or phenyl for **7m** (EC_{50} = 0.07 μM) or hetero aliphatic ring **7n** (EC_{50} = 0.37 μM). As shown in Table 2 compound **7m** led to an increase in activity with an EC_{50} better than the reference compound **2a**.

Interestingly, compound **7o** which contained a phenyl group at the *meta*-position showed moderate activity (EC_{50} = 0.25 μM) compared with compound **7m** where the same group was at the *para* position, in line with our expectations.

On the contrary, moving the methoxy group from the *para* **7h** to the *ortho* **7p** and to the *meta* position **7q** led to a significant increase in activity (EC_{50} = 0.14 μM and EC_{50} = 0.10 μM).

A similar trend was observed using a bromine in the *meta* position **7r** (EC_{50} = 0.18 μM) which was better than the para position (see **7b** EC_{50} = 0.53 μM in Table 2). Changing the bromine to fluorine in the *meta* position caused increased potency in **7s**

Table 2
Chemical structure and potency profile of the novel hybrids **7a**-**7z** as F508del CFTR correctors.

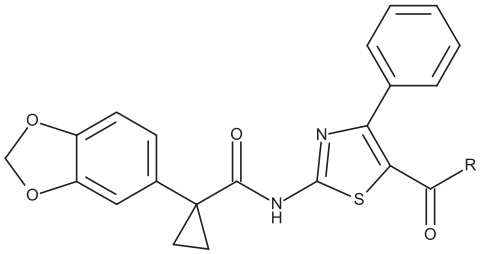

Compound	R	EC_{50} (μM)
7a	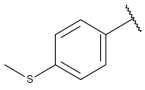	0.10
7b	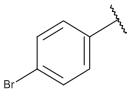	0.53
7c	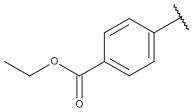	0.41
7d	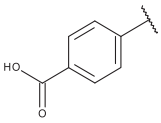	7.31
7e	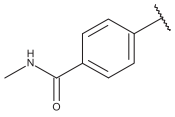	NA
7f	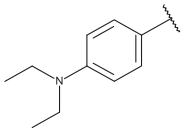	0.21
7g	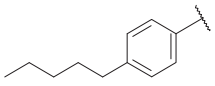	0.43
7h	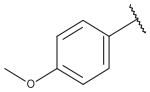	0.45
7i	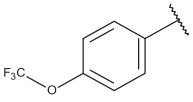	0.36
7j	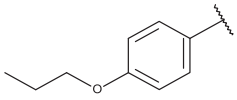	0.017
7k	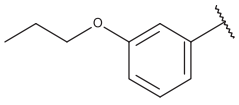	0.16
7l	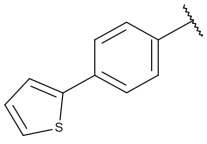	1.06

Table 2 (*continued*)

Compound	R	EC_{50} (μM)
7m	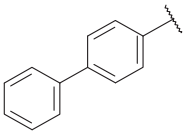	0.07
7n	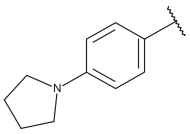	0.37
7o	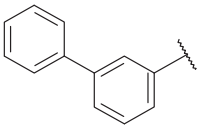	0.25
7p	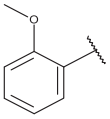	0.14
7q	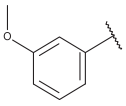	0.10
7r	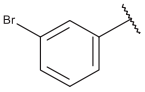	0.18
7s	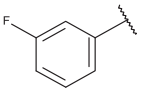	0.13
7t	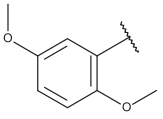	0.11
7u	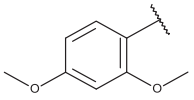	0.40
7v	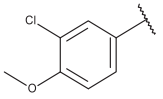	0.41
7w	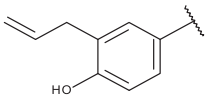	0.28
7x	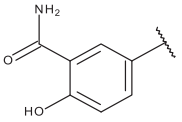	13.70
7y	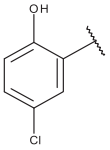	1.60
7z	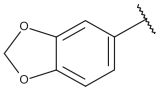	0.11

Table 3
Chemical structure and potency profile of the novel hybrids **24a**-**24c** as F508del CFTR correctors.

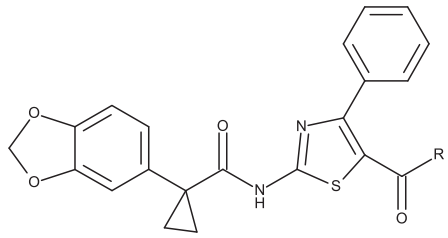

Compound	R	EC_{50} (μM)
24a	CH_3	2.72
24b	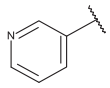	0.79
24c	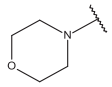	8.50

(EC_{50} = 0.13 μM).

Given the inclination of the methoxy group for the *meta/ortho* substitution, we synthesized two disubstituted analogues which contain the methoxy group in the *ortho* position and the second one in the *meta* and *para* position respectively (**7t** and **7u**). Interestingly, while 4-substitution wasn't well tolerated (EC_{50} = 0.4 μM), inclusion of a 3′-OCH_3 group afforded potent analogue (EC_{50} = 0.11 μM).

Indeed, we evaluated molecules containing 3, 4-substitued benzoyl groups like **7v** (EC_{50} = 0.41 μM or **7w** (EC_{50} = 0.28 μM). In these cases, the substitution proved to be tolerated, especially with regard to the allyl moiety. On the other hand, a high decrease in activity was observed when one of these substituents was an amide group as in **7x** (EC_{50} = 13.7 μM) and similarly with **7e**. From the above SAR, it was identified that an amide group was detrimental for activity.

Moreover, we decided to test **7y**, another derivative containing 2′,5′-substitued benzoyl groups, considering that compound **7t** containing two methoxy groups in same positions was active (EC_{50} = 0.11 μM).

The replacement of methoxy groups with chlorine and hydroxyl displayed about 15-fold loss of potency (EC_{50} = 1.6 μM)**.** This may indicate that an electron-donating group like −OCH_3 at the *meta* position was favorable (see **7q** and **7t**).

A particular compound containing a dioxane moiety **7z** was at last analyzed. The compound exhibited good corrector ability (EC_{50} = 0.10 μM) rather similar to that of the lead compound.

All the compounds in the libraries contain at the 5 position only a benzoyl derivative. We tried to insert a different keto group using aliphatic like methyl **24a**, heteroaromatic like pyridine **24b** and heterocycle, morpholine in this case, **24c** in the same position. Only **24b** (EC_{50} = 0.79 μM) had a certain activity while **24a** (EC_{50} = 2.72 μM) and overall **24c** (EC_{50} = 8.5 μM) led to decreasing activity with respect to the progenitor (EC_{50} = 0.087 μM) as appeared in Table 3.

The ability of the novel derivates to rescue F508del-CFTR was assayed on well-differentiated primary cultures of human bronchial epithelial cells from a CF patient homozygous for the F508del mutation, using an electrophysiological technique: the trans epithelial electrical resistance and potential difference measurements (TEER/PD). We tested **7a** and **7m**, two of the most potent derivates described in this study. Epithelia were treated for 24 h with test compounds at different concentrations: **7a** (5−0.5−0.05 μM), **7m** (10 - 1−0.1 μM), VX-809 1 μM (as positive control) or vehicle alone (DMSO; negative control) and then assayed. Trans epithelial electrical resistance was measured before and after stimulation with forskolin (20 μM) plus genistein (50 μM) to totally activate CFTR. It was then measured after addition of the CFTR inhibitor PPQ-102 (30 μM) to fully block CFTR activity. The bar graphs of Fig. 5 show the delta between the values of electrical resistance measured before and after CFTR inhibition, converted into its reciprocal conductance. Long-term treatment of CF primary bronchial epithelia with **7a** and **7m** significantly increased both CFTR-mediated conductance and equivalent short-circuit current.

We then evaluated the rescue of processing defect biochemically by means of the electrophoretic mobility of CFTR protein. In Western blots, CFTR protein is detected as two bands, named B and C, of approximately 150 and 170 kDa, respectively. Band B corresponds to partially glycosylated CFTR residing in the ER, while band C is the fully processed (mature) CFTR that has passed through the Golgi. The prevalent form in cells expressing wild-type CFTR is band C. Lysates of cells expressing F508del-CFTR show primarily band B, consistent with the severe trafficking defect caused by the mutation (Fig. 6A). To evaluate the effect of hybrid compounds on CFTR electrophoretic mobility, we treated F508del-CFTR/HS-YFP expressing CFBE41o-cells with DMSO (vehicle alone) or test compounds **7m** and **7a** (0.5 μM) or VX-809 (1 μM, as positive control). After 24 h, cells were lysed and lysates were subjected to SDS-PAGE followed by western blotting. Western blot images were analyzed with ImageJ software. For each lane, CFTR bands, analyzed as ROI, were quantified after normalization for GAPDH to account for total protein loading. Treatment of F508del-CFTR cells with corrector VX-809 significantly enhanced expression of mature CFTR (band C), resulting in a change in the C band/B band ratio. Similarly, treatment with the compounds resulted in a significant increase in the C band/B band ratio, comparable to that obtained following treatment with VX-809 (Fig. 6B).

To further characterize the biological activity of hybrid compounds, we tested **7a, 7j, 7m** in combination with VX-809 and VX-661, in CFBE41o-cells stably expressing F508del-CFTR by means of the YFP functional assay (Supporting **information S5**). To this aim, cells were treated for 24 h with single test compounds or their

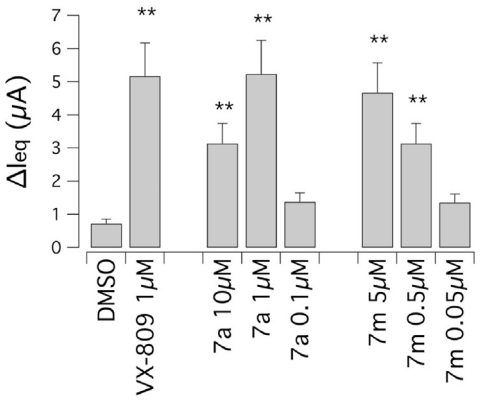

Fig. 5. Compounds **7a** and **7m** rescue F508del-CFTR activity in primary bronchial epithelia. The graph reports the equivalent short-circuit current (calculated from TEER/PD measurements) in F508del/F508del bronchial epithelia, treated for 24 h with test compounds at the indicated concentration, or VX-809 (1 μM), or vehicle alone (DMSO). Data are expressed as means ± SD, n = 3.

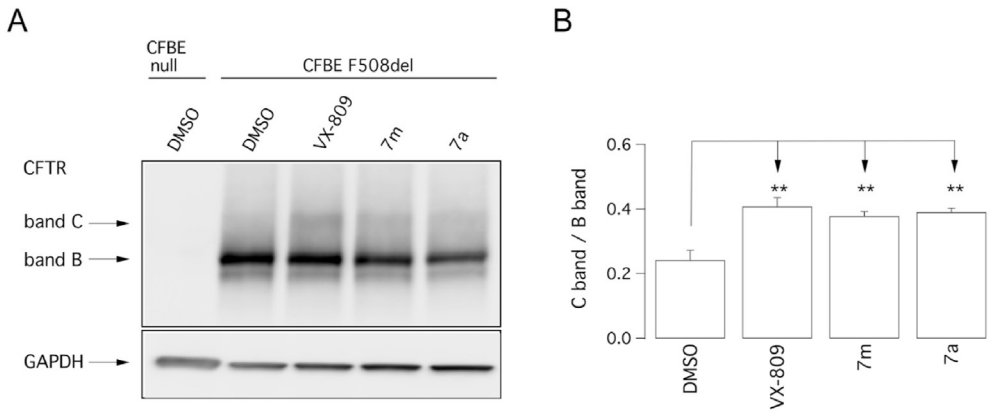

Fig. 6. Biochemical analysis of the F508del-CFTR expression pattern. (A) Electrophoretic mobility of F508del-CFTR in 2 different preparations of CFBE41o-cells, treated for 24 h with vehicle or test compounds (0.5 μM) or VX-809 (1 μM). Arrows indicate complex-glycosylated (band C) and core-glycosylated (band B) forms of CFTR protein. (B) The bar graph reports the densitometric analysis (means ± SEM, n = 3) of band C/band B ratio normalized to GAPDH. **P < 0.01 versus control (ANOVA with Dunnett's post hoc test).

combinations and then assayed. No additive or synergistic effect was observed when combining **7a, 7j** and **7m** with VX-809 or VX-661, supporting the hypothesis that all these compounds possibly share the same binding site (Supporting **information S5**).

2.4. Evaluation of the effective capacity of the compounds to bind F508del-CFTR

When a compound shows F508del-CFTR rescuing-activity in cell models, it is important to rule out off-target effects demonstrating that its mechanism of action corresponds to a direct interaction with the mutated protein. We then decided to evaluate the effective capacity of **7j** and of **7m** to bind to F508del-CFTR exploiting the biosensor recently described by us in which the mutated protein was immobilized in membrane-like lipid vesicles as to resemble the F508del-CFTR environment in vivo [38]. Injection of increasing concentrations of **7j** and of **7m** onto the biosensor containing F508del-CFTR provided saturable and dose-dependent binding curves (Fig. 7) that permitted the calculation of Kd values equal to 38.2 ± 5.1 and 89.3 ± 35.3 μM for the two compounds respectively. In the same experimental condition, VX-809, here used as a positive control, bound F508del-CFTR with similar affinity (Kd value equal to 72.8 ± 19.5 μM) [33]. Thus, in agreement with docking results, **7j** and **7m** effectively set up a high affinity complex with F508del-CFTR that is responsible for the functional rescue of the mutated channel.

2.5. Molecular docking studies

The results of our docking calculations support the aforementioned SAR discussion underlining a key role played by the introduction of hydrophobic groups onto the para position of the benzoyl moiety as highly effective to achieve corrector ability. On the other hand, the selection of 3,4-substitued benzoyl groups proved to be well-tolerated, especially in presence of electron-rich groups (see **7v** and **7w**). This was motivated by the proper conformation displayed by the corrector, which is able to interact efficiently with E656 and to exhibit contacts with Y577. Accordingly, the most potent compound **7j** displayed a highly similar docking positioning with those previously discussed for VX-809 and SUL-809, giving further validation of the relevance of bulky, flexible and quite lipophilic groups linked at the benzoyl moiety. As shown in Fig. 8, the benzodioxole moiety of the new corrector is H-bonded to G461, K464 and T465, while the oxygen atom of the benzoyl group displays contacts with the backbone of E656. Notably, the propoxy group of **7j** features hydrophobic contacts with the aromatic ring of Y577, being able to reproduce the positioning experienced by the sulfonamide group of SUL-809.

This kind of docking mode was shared by most of the other promising hybrids, such as **7a** featuring a thiomethyl group onto the *para* position of the benzoyl substituent (Supporting **information S6**), while the analogue **7m** bearing the biaryl moiety as bioisoster of the 4-(methylthio)benzoyl group displayed a switched positioning (Fig. 9). This was in agreement with the docking pose previously discussed for the first series of hybrids such as for **2b** (Supporting **information S3**), featuring **7m** in any case the recurrent previously cited contacts displayed by the benzodioxolane ring and H-bonds with Y577.

Conceivably, this docking mode is probably due to steric hindrance caused by the bulky biaryl substituent selected for this hybrid. In any case, this positioning allowed maintaining the aforementioned key contacts with N659, K464 and T465 while interaction with E656 or Y577 appeared to be both involved in stabilizing the corrector at the hNBD1 domain (Fig. 9).

3. Conclusion

In this work, we successfully applied a multi-disciplinary approach in order to identify a new series of hybrid compounds displaying promising F508del-CFTR corrector ability. Preliminary molecular docking studies performed on VX-809 and **2a** revealed the most substantial key feature involved in corrector binding, guiding the design of the second series of hybrids featuring structural variations of the benzoyl group of the prototype **2a**. Based on computational predictions, the most promising compounds had been synthesized and evaluated as correctors of F508del-CFTR trafficking defect. SPR results experimentally validated the compound binding to CFTR protein, supporting the effectiveness of **7j** and **7m** as optimized F508del-CFTR corrector hybrids. On the whole, molecular docking of the newly synthesized correctors revealed H-bonding K464, T465 and N659 through the benzodioxole moiety and the carboxamide function as the necessary molecular requirements identified within hybrids. However, hydrophobic contacts with the protein pocket delimited by Y577 and E656 allowed improving the corrector potency. A dedicated site-specific mutagenesis program will represent the prosecution of this study to validate the results from our multi-disciplinary approach.

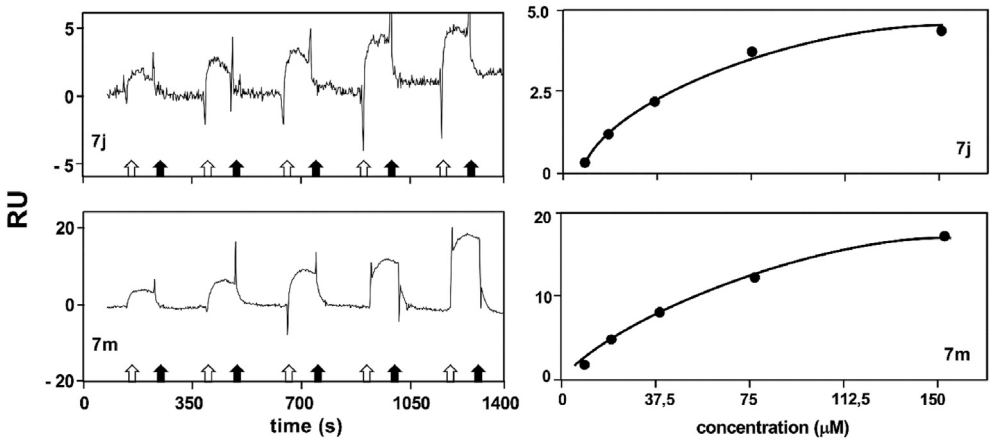

Fig. 7. Left panels: Blank-subtracted sensorgrams derived from a single cycle analysis of **7j** (upper panel) or of **7m** (lower panel) both at 9.4, 18.8, 40, 37.5, 75, 150 μM injected on the F508del-CFTR biosensor. White and black arrows point to the start and end of the injections, respectively. Right panels: Steady-state analysis of **7j** (upper panel) or of **7m** (lower panel) injected onto the F508del-CFTR-containing biosensor (same doses as above). The results shown are representative of other three that gave similar results.

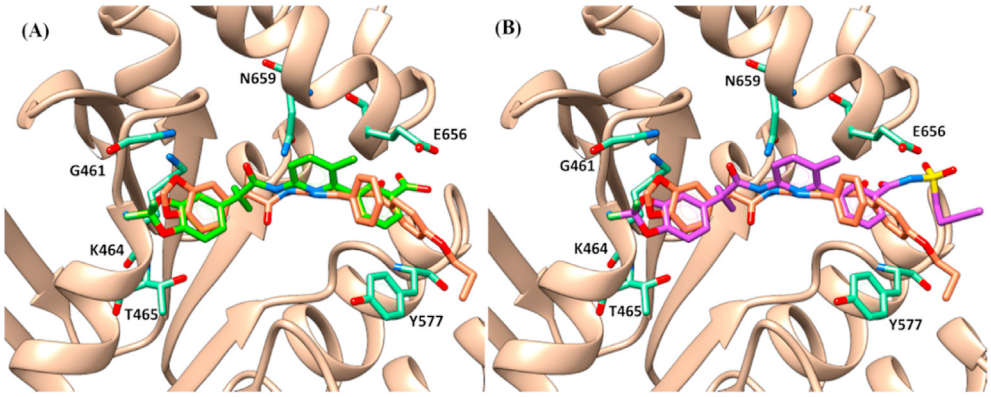

Fig. 8. Docking mode of **7j** (C atom; orange) in comparison with that of VX-809 (*C* atom; light green) (A) and of SUL-809 (*C* atom; purple) (B) at the hNBD1 domain of the F508del CFTR mutant. (For interpretation of the references to color in this figure legend, the reader is referred to the Web version of this article.)

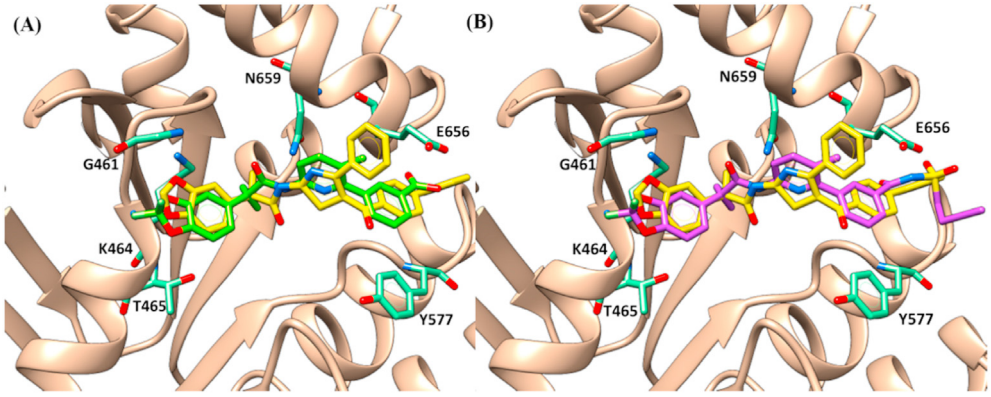

Fig. 9. Docking mode of **7m** (*C* atom; yellow) in comparison with that of VX-809 (*C* atom; light green) (A) and of SUL-809 (*C* atom; purple) (B) at the hNBD1 domain of the F508del CFTR mutant. (For interpretation of the references to color in this figure legend, the reader is referred to the Web version of this article.)

4. Experimental

4.1. Chemistry

Reagents and solvents were purchased from Sigma Aldrich, Alfa Aesar, VWR and Zentek used as received unless otherwise indicated.

Solvent removal was accomplished with a rotary evaporator at ca.10−50 Torr. The analytical instrument used was an Agilent 1260 high performance liquid chromatography (HPLC). The analytical HPLC column was a Phenomenex C18 Luna (4.6 × 250 mm, 5 μm).

The preparative HPLC was Agilent 1260 Infinity preparative HPLC and the column used for preparative chromatography was a Phenomenex C18 Luna (21.2 × 250 mm, 15 μm). The analysis of the

intermediates and the raw products was performed by liquid chromatography-electrospray mass spectrometry (HPLC-ESI-MS) using an Agilent 1100 series LC/MSD ion trap instrument.

HRMS experiments were performed using Q Exactive Orbitrap instrument by Thermo Scientific.

The nuclear magnetic resonance (NMR) spectrometer was a Varian Gemini 200 MHz.

The proton spectra were acquired at 200 MHz while carbon spectra were acquired at 50 MHz, at room temperature. Chemical shifts are reported in δ units (ppm) relative to TMS as an internal standard. Coupling constants (J) are reported in Hertz (Hz).

All the raw powders obtained were purified with preparative HPLC using the following gradient: from 0 to 5 min at 20% eluent B, then from 5 min to 40 min to 100% eluent B, from 40 to 45 min at 100% eluent B. Eluent A was water with 0.1% formic acid (FOA) and eluent B was acetonitrile with 0.1% FOA. All analogues submitted for testing were judged to be of 95% or higher purity based on analytical HPLC/MS analysis.

Compound purity was determined by integrating peak areas of the liquid chromatogram, monitored at 254 nm.

*4.1.1. 1-(Benzo[d][1,3]dioxol-6-yl)-N-(5-(4-(methylthio)benzoyl)-4-phenylthiazol-2-yl)cyclo propanecarboxamide (**7a**)*

A mixture of (4-methoxyphenyl) methanamine (535 μL, 4 mmol) and 4-(methoxy)benzaldehyde (595 μL, 4.8 mmol) in methanol (2 mL) was heated to reflux for 3 h, then cooled to T = 0 °C, $NaBH_4$ (228 mg, 6 mmol) was added portion wise to the reaction and the resulting mixture was stirred at room temperature for about 10 h. Solvent was removed under reduced pressure and the residue was partitioned between ethyl acetate (EtOAc) and H_2O. The combined organic layers were washed with H_2O, and then dried over anhydrous Na_2SO_4. After filtration, solvent was removed in vacuum to afford bis [4-methoxyphenyl]methylamine (962 mg, 94%) as a colorless oil which was used in the next step without further purification. ESI-MS: *m/z* 258.0 $[M+H]^+$.

To a solution of benzoylisothiocyanate (140 μL, 1 mmol) in acetone (1 mL) cooled at T = 0 °C, bis [4-methoxyphenyl]methylamine (257 mg, 1 mmol) in acetone (1 mL) was added at this temperature and stirred for an additional 1 h.

The mixture was concentrated under reduced pressure, to afford *N*-(bis(4-methoxybenzyl) carbamothioyl)benzamide (398 mg, 95%) as yellow sticky oil which was used in the next step without further purification. ESI-MS: *m/z* 421.0 $[M+H]^+$.

A solution of 2-bromo-1-(4-(methylthio)phenyl)ethanone (123 mg, 0.5 mmol) and *N*-(bis(4-methoxybenzyl)carbamothioyl)-benzamide (210 mg, 0.5 mmol) in N, *N*-dimethylformamide (DMF) (3 mL) was stirred at T = 85 °C for 3 h. After cooling to room temperature, the mixture was partitioned between EtOAc and H_2O. The organic layer was washed with brine and dried over anhydrous Na_2SO_4. After filtration, solvent was removed in vacuum and the residue was stirred in trifluoroacetic acid (TFA) (4 mL) at T = 80 °C for 24–36 h until complete deprotection. Most of TFA was removed under reduced pressure. The residue was then neutralized with $NaHCO_3$ 1 N, and then extracted with EtOAc for 3 times. The combined organic layers were washed with brine and dried over anhydrous Na_2SO4. After filtration, the solution was concentrated and further crystallized in acetonitrile to afford (2-amino-4-phenylthiazol-5-yl) (4-(methylthio)phenyl) methanone (127 mg, 78%) as a brown solid. ESI-MS: *m/z* 328.1 $[M+H]^+$.

Benzo [1,3]dioxol-5-yl-cyclopropanecarboxylic acid (20.6 mg, 0.1 mmol) was resuspended in anhydrous DMF (1 mL); HATU (38 mg, 0.1 mmol) and DIPEA (35 μL, 0.2 mmol) were added. The reaction was vigorously stirred for 5 min and (2-amino-4-phenylthiazol-5-yl) (4-(methylthio) phenyl) methanone (32.7 mg, 0.1 mmol) in anhydrous DMF (500 mL) was added. The reaction was kept at T = 50 °C until completeness (18–24 h) and then purified by preparative HPLC. The peak of interest was concentrated to obtain the title compound as yellow solid with purity of >95% as determined by HPLC-MS (12.7 mg, 25%).

^1H NMR (200 MHz, DMSO-d_6): δ 11.89 (s, broad, 1H, NH); 7.71–6.57 (m, 12H, arom); 6.02 (s, 2H OCH_2O); 2.37 (s, 3H, SCH 3); 1.68–1.42 (m, 2H, CH_2, cyclopr); 1.40–1.09 (m, 2H, CH_2, cyclopr).

^{13}C NMR (50 MHz, DMSO-d_6): δ 187.3, 165.7, 158.6, 153.9, 146.9, 146.3, 131.8, 130.9, 129.6, 128.9, 128.1, 127.4, 123.1, 114.5, 110.2, 107.8, 100.6, 98.7, 51.8, 30.3, 15.5.

HRMS (ESI) calculated for $C_{28}H_{23}N_2O_4S_2$: $[M + H]^+$ 515.10992; found 515.10971.

*4.1.2. 1-(Benzo[d][1,3]dioxol-5-yl)-N-(5-(4-bromobenzoyl)-4-phenylthiazol-2 yl)cyclopropanecarboxamide (**7b**)*

Compound **7b** (17.5 mg, 32%) was prepared from (2-amino-4-phenylthiazol-5-yl) (4-bromophenyl)methanone (35.9 mg, 0.1 mmol) and benzo [1,3]dioxol-5-yl-cyclopropanecarboxylic acid (20.6 mg, 0.1 mmol) in the same manner as described for **7a** as brown solid.

^1H NMR (200 MHz, DMSO-d_6) δ 12.02 (s, 1H, NH), 7.68–6.91 (m, 12H, arom), 6.06 (s, 2H, OCH_2O), 1.72–1.44 (m, 2H, CH_2, cyclopr), 1.38–1.12 (m, 2H, CH_2, cyclopr).

^{13}C NMR (50 MHz, DMSO-d_6) δ, 187.8, 172.4, 160.2, 154.5, 146.9, 146.3, 136.3, 133.6, 131.8, 130.7, 130.6, 129.2, 128.3, 127.4, 125.8, 124.1, 123.3, 110.2, 107.8, 100.6, 30.3, 15.5.

HRMS (ESI) calculated for $C_{27}H_{20}BrN_2O_4S$: $[M + H]^+$ 547.03271; found 547.03215.

*4.1.3. Ethyl4-(2-(1-(benzo[d][1,3]dioxol-5-yl) cyclopropanecarboxamido)-4-phenylthiazole-5-carbonyl)benzoate (**7c**)*

Compound **7c** (18.4 mg, 34%) was prepared from ethyl 4-(2-amino-4-phenylthiazole-5-carbonyl) benzoate (35.2 mg, 0.1 mmol) and benzo [1,3]dioxol-5-yl-cyclopropanecarboxylic acid (20.6 mg, 0.1 mmol) in the same manner as described for **7a** as brown solid.

^1H NMR (200 MHz, DMSO-d_6): δ 12.05 (s, broad, 1H, NH), 7.84–6.82 (m, 12H, arom), 6.03 (s, 2H OCH_2O), 4.45 (q, J = 7.2, 2H, $O\underline{CH_2}CH_3$), 1.67–1.48 (m, 2H, CH_2, cyclopr), 1.41–1.04 (5H, m, 2H, CH_2, cyclopr + superimposed t, J = 7.2, 3H, $OCH_2\underline{CH_3}$).

^{13}C NMR (50 MHz, DMSO-d_6): δ 188.2, 172.5, 164.5, 160.5, 155.0, 146.9, 146.3, 141.1, 133.6, 131.9, 131.7, 129.5, 128.7, 128.3, 128.2, 127.3, 124.3, 123.2, 110.2, 107.8, 100.6, 60.7, 30.3, 15.5, 13.6.

HRMS (ESI) calculated for $C_{30}H_{25}N_2O_6S$: $[M + H]^+$ 541.14332; found 541.14314.

*4.1.4. 4-(2-(1-(Benzo[d][1,3] dioxol-5-yl) cyclopropanecarboxamido)-4-phenylthiazole-5-carbonyl) benzoic acid (**7d**)*

Compound **7d** (9.9 mg, 19%) was prepared from 4-(2-amino-4-phenylthiazole-5-carbonyl)benzoic acid (32.4 mg, 0.1 mmol) and benzo [1,3]dioxol-5-yl-cyclopropanecarboxylic acid (20.6 mg, 0.1 mmol) in the same manner as described for **7a** as brown solid.

^1H NMR (200 MHz, DMSO-d_6): δ 13.18 (s, 1H, broad, COOH); 11.99 (s, broad, 1H, NH); 8.02–6.73 (m, 12H, arom); 6.03 (s, 2H OCH_2O); 1.68–1.43 (m, 2H, CH_2, cyclopr); 1.40–1.05 (m, 2H, CH_2, cyclopr).

^{13}C NMR (50 MHz, DMSO-d_6): δ 187.7, 171.6, 168.8, 154.6, 146.9, 146.3, 137.0, 131.3, 130.2, 129.4, 128.7, 128.2, 127.5, 123.1, 113.1, 110.2, 107.8, 100.6, 30.3, 15.5.

HRMS (ESI) calculated for $C_{28}H_{21}N_2O_6S$: $[M + H]^+$ 513.11202; found 513.11179.

*4.1.5. 4-(2-(1-(Benzo[d] [1,3]dioxol-5-yl) cyclopropanecarboxamido)-4-phenylthiazole-5-carbonyl)-N-methylbenzamide (**7e**)*

Compound **7e** (12 mg, 11%) was prepared from 4-(2-amino-4-phenylthiazole-5-carbonyl)-*N*-methylbenzamide (68 mg, 0.2 mmol) and benzo [1,3]dioxol-5-yl-cyclopropanecarboxylic acid (41 mg, 0.20 mmol) in the same manner as described for **7a** as brown oil.

^{1}H NMR (200 MHz, DMSO-d_6): δ 12.01 (s, 1H, broad, NH); 11.75 (s, broad, 1H, NH); 7.71–6.63 (m, 12H, arom); 6.03 (s, 2H OCH_2O); 2.43 (s, 3H, CH_3N); 1.72–1.46 (m, 2H, CH_2, cyclopr); 1.42–1.11 (m, 2H, CH_2, cyclopr).

^{13}C NMR (50 MHz, DMSO-d_6): δ 187.8, 172.3, 167.8, 154.1, 146.8, 146.3, 136.6, 131.8, 130.3, 129.3, 128.8, 128.1, 127.5, 123.2, 113.5, 110.2, 107.8, 100.6, 38.5, 30.3, 15.5.

HRMS (ESI) calculated for $C_{29}H_{24}N_3O_5S$:[M + H]$^+$ 526.14366; found 526.14343.

*4.1.6. 1-(Benzo[d][1,3]dioxol-5-yl)-N-(5-(4-(diethylamino) benzoyl)-4-phenylthiazol-2-yl) cyclopropanecarboxamide (**7f**)*

Compound **7f** (12.5 mg, 23%) was prepared from (2-amino-4-phenylthiazol-5-yl) (4-(diethylamino) phenyl)methanone (35 mg, 0.1 mmol) and benzo [1,3]dioxol-5-yl-cyclopropanecarboxylic acid (20.6 mg, 0.1 mmol) in the same manner as described for **7a** as white solid.

^{1}H NMR (200 MHz, DMSO-d_6): δ 11.94 (s, broad, 1H, NH), 7.79–6.85 (m, 12H, arom), 6.05 (s, 2H OCH_2O), 2.83 (q, 4H, J = 6.8, NCH_2), 1.65–1.41 (m, 2H, CH_2, cyclopr), 1.40–1.09 (m, 2H, CH_2, cyclopr), 1.04 (t, 6H, J = 6.8, $\underline{CH_3}CH_2N$).

^{13}C NMR (50 MHz, DMSO-d_6): δ 188.3, 172.3, 163.2, 160.6, 155.2, 146.9, 146.3, 134.2, 133.7, 131.9, 131.6, 129.2, 128.7, 128.3, 128.1, 127.4, 124.3, 123.1, 110.2, 107.8, 100.6, 51.8, 30.3, 15.5, 13.8.

HRMS (ESI) calculated for $C_{31}H_{30}N_3O_4S$: [M + H]$^+$ 540.19569; found 540.19544.

*4.1.7. 1-(Benzo[d][1,3]dioxol-5-yl)-N-(5-(4-pentylbenzoyl)-4-phenylthiazol-2-yl) cyclopropanecarboxamide (**7g**)*

Compound **7g** (13.5 mg, 25%) was prepared from (2-amino-4-phenylthiazol-5-yl) (4-pentylphenyl)methanone (35 mg, 0.1 mmol) and benzo [1,3]dioxol-5-yl-cyclopropanecarboxylic acid (20.6 mg, 0.1 mmol) in the same manner as described for **7a** as pale yellow solid.

^{1}H NMR (200 MHz, DMSO-d_6): δ 11.90 (s, broad, 1H, NH), 7.61–6.76 (m, 12H, arom), 6.05 (s, 2H OCH_2O), 1.65–1.42 (m, 2H, CH_2, cyclopr), 1.41–1.05 (m, 6H, 2H, CH_2, cyclopr + 4H, CH_2CH_2), 0.98–0.72 (m, 7H, $CH_2CH_2CH_3$).

^{13}C NMR (50 MHz, DMSO-d_6): δ 188.4, 172.3, 159.5, 174.2, 146.9, 146.3, 134.8, 133.8, 131.8, 128.9, 128.8, 128.0, 127.6, 127.3, 124.3, 123.2, 110.2, 107.8, 100.6, 34.5, 30.3, 30.1, 29.7, 28.5, 21.5, 15.4, 13.4.

HRMS (ESI) calculated for $C_{32}H_{31}N_2O_4S$: [M + H]$^+$ 539.20044; found 539.20018.

*4.1.8. 1-(Benzo[d][1,3]dioxol-5-yl)-N-(5-(4-methoxybenzoyl)-4-phenylthiazol-2-yl) cyclopropanecarboxamide (**7h**)*

Compound **7h** (18.9 mg, 38%) was prepared from (2-amino-4-phenylthiazol-5-yl) (4-methoxyphenyl)methanone (31 mg, 0.1 mmol) and benzo [1,3]dioxol-5-yl-cyclopropanecarboxylic acid (20.6 mg, 0.1 mmol) in the same manner as described for **7a** as brown solid.

^{1}H NMR (200 MHz, DMSO-d_6): δ 11.80 (s, broad, 1H, NH), 7.78–6.92 (m, 12H, arom), 6.04 (s, 2H OCH_2O), 3.76 (s, 3H, OCH_3), 1.63–1.42 (m, 2H, CH_2, cyclopr), 1.41–1.16 (m, 2H, CH_2, cyclopr).

^{13}C NMR (50 MHz, DMSO-d_6): δ 187.2, 162.5, 159.0, 154.8, 146.9, 146.3, 131.8, 131.2, 129.7, 128.8, 128.1, 127.5, 123.2, 113.1, 110.2, 107.8, 100.6, 97.2, 55.1, 30.2, 15.4.

HRMS (ESI) calculated for $C_{28}H_{23}N_2O_5S$: [M + H]$^+$ 499.13276; found 499.13224.

*4.1.9. 1-(Benzo[d][1,3]dioxol-5-yl)-N-(4-phenyl-5-(4-(trifluoromethoxy)benzoyl)thiazol-2-yl) cyclopropanecarboxamide (**7i**)*

Compound **7i** (12.5 mg, 23%) was prepared from (2-amino-4-phenylthiazol-5-yl) (4-(trifluoromethoxy)phenyl)methanone (36 mg, 0.1 mmol) and benzo [1,3]dioxol-5-yl-cyclopropanecarboxylic acid (20.6 mg, 0.1 mmol) in the same manner as described for **7a** as pale brown solid.

^{1}H NMR (200 MHz, DMSO-d_6): δ 12.03 (s, broad, 1H, NH), 7.76–6.79 (m, 12H, arom), 6.05 (s, 2H OCH_2O), 1.65–1.43 (m, 2H, CH_2, cyclopr), 1.41–1.04 (m, 2H, CH_2, cyclopr).

^{13}C NMR (50 MHz, DMSO-d_6): δ 187.6, 172.5, 160.4, 154.9, 146.9, 146.3, 136.3, 133.6, 131.7, 130.8, 129.2, 128.2, 127.2, 124.4, 123.2, 119.8, 110.2, 107.8, 100.6, 30.3, 15.5.

HRMS (ESI) calculated for $C_{28}H_{20}F_3N_2O_5S$: [M + H]$^+$ 553.10449; found 553.10404.

*4.1.10. 1-(Benzo[d][1,3]dioxol-5-yl)-N-(4-phenyl-5-(4-propoxybenzoyl)thiazol-2-yl) cyclopropanecarboxamide (**7j**)*

Compound **7j** (9.6 mg, 18%) was prepared from (2-amino-4-phenylthiazol-5-yl) (4-propoxyphenyl) methanone (34 mg, 0.1 mmol) and benzo [1,3]dioxol-5-yl-cyclopropanecarboxylic acid (20.6 mg, 0.1 mmol) in the same manner as described for **7a** as pale yellow solid.

^{1}H NMR (200 MHz, DMSO-d_6): δ 11.94 (s, broad, 1H, NH); 7.65–6.58 (m, 12H, arom); 6.01 (s, 2H OCH_2O); 3.93 (t, 2H, J = 7.0, $O\underline{CH_2}CH_2$); 1.85–1.44 (m, 4H, 2H, $OCH_2\underline{CH_2}$, + 2H, CH_2, cyclopr); 1.41–1.09 (m, 2H, CH_2, cyclopr); 0.96 (t, 3H, J = 7.0, $CH_2\underline{CH_3}$).

^{13}C NMR (50 MHz, DMSO-d_6): δ 178.1, 164.7, 156.5, 153.8, 146.9, 146.4, 132.2, 131.3, 129.6, 128.9, 128.2, 127.5, 123.1, 113.6, 110.2, 107.8, 100.6, 99.2, 57.8, 30.3, 22.7, 15.4.

HRMS (ESI) calculated for $C_{30}H_{27}N_2O_5S$: [M + H]$^+$ 527.16406; found 527.16388.

*4.1.11. 1-(Benzo[d][1,3]dioxol-5-yl)-N-(4-phenyl-5-(3-propoxybenzoyl)thiazol-2 yl)cyclopropanecarboxamide (**7k**)*

3-(Prop-1-yloxy)acetophenone (356 mg, 2 mmol) synthetized starting from 3-hydroxyacetophenone as previously described [39], was brominated with $CuBr_2$ using the general procedure previously described [40] providing 2-bromo-1-(3-propoxyphenyl)ethanone intermediate (460 mg, 90%). The purity was verified by HPLC-MS without further purification.

A solution of 2-bromo-1-(3-propoxyphenyl)ethanone (128 mg, 0.5 mmol) and *N*-(bis(4-methoxybenzyl)carbamothioyl)-benzamide (210 mg, 0.5 mmol) in DMF (3 mL) was stirred at T = 85 °C for 3 h according to the protocol for compound **7a**. After TFA deprotection and crystallization in acetonitrile (2-amino-4-phenylthiazol-5-yl) (3-propoxyphenyl)methanone (118 mg, 70%) was isolated. ESI-MS: *m/z* 339.1 [M+H]$^+$.

(2-Amino-4-phenylthiazol-5-yl) (3-propoxyphenyl)methanone (34 mg, 0.1 mmol) and benzo [1,3] dioxol-5-ylcyclopropanecarboxylic acid (20.6 mg, 0.1 mmol) was then conjugated in the same manner as described for **7a** to furnish, after HPLC purification, the title compound as pale brown oil (11 mg, 21%).

HRMS (ESI) calculated for $C_{30}H_{27}N_2O_5S$: [M + H]$^+$ 527.16406; found 527.16385.

*4.1.12. 1-(Benzo[d][1,3]dioxol-5-yl)-N-(4-phenyl-5-(4-(thiophen-2-yl)benzoyl)thiazol-2-yl) cyclopropanecarboxamide (**7l**)*

Compound **7l** (11.7 mg, 21%) was prepared from (2-amino-4-phenylthiazol-5-yl) (4-(thiophen-2-yl) phenyl)methanone

(36.2 mg, 0.1 mmol) and benzo [1,3]dioxol-5-yl-cyclopropanecarboxylic acid (20.6 mg, 0.1 mmol) in the same manner as described for **7a** as brown oil.

^{1}H NMR (200 MHz, DMSO-d_6): δ 11.96 (s, 1H, broad, NH); 7.95–6.73 (m, 15H, arom); 6.04 (s, 2H OCH_2O); 1.73–1.42 (m, 2H, CH_2, cyclopr); 1.40–1.05 (m, 2H, CH_2, cyclopr).

^{13}C NMR (50 MHz, DMSO-d_6): δ 176.8, 172.1, 159.7, 154.3, 146.9, 146.2, 137.6, 137.0, 133.4, 131.7, 131.3, 129.6, 128.8, 128.2, 127.5, 123.2, 113.4, 110.2, 107.8, 100.6, 30.3, 15.5.

HRMS (ESI) calculated for $C_{31}H_{23}N_2O_4S_2$: $[M + H]^+$ 551.10992; found 551.10971.

4.1.13. N-(5-([1,1′-biphenyl]-4-carbonyl)-4-phenylthiazol-2-yl)-1-(benzo[d][1,3]dioxol-5-yl) cyclopropanecarboxamide ***(7m)***

Compound **7m** (15.3 mg, 28%) was prepared from [1, 1′-biphenyl]-4-yl (2-amino-4-phenylthiazol-5-yl)methanone (35.7 mg, 0.1 mmol) and benzo [1,3]dioxol-5-yl-cyclopropanecarboxylic acid (20.6 mg, 0.1 mmol) in the same manner as described for **7a** as pale yellow solid.

^{1}H NMR (200 MHz, DMSO-d_6): δ 12.01 (s, 1H, broad, NH); 7.92–6.76 (m, 17H, arom); 6.05 (s, 2H OCH_2O); 1.78–1.44 (m, 2H, CH_2, cyclopr); 1.42–1.08 (m, 2H, CH_2, cyclopr).

^{13}C NMR (50 MHz, DMSO-d_6): δ 188.2, 172.2, 156.8, 153.2, 146.9, 146.3, 140.7, 137.9, 133.2, 131.3, 129.3, 128.9, 128.2, 127.4, 123.1, 110.2, 107.8, 100.6, 30.3, 15.4.

HRMS (ESI) calculated for $C_{33}H_{25}N_2O_4S$: $[M + H]^+$ 545.15349; found 545.13351.

4.1.14. 1-(Benzo[d][1,3]dioxol-5-yl)-N-(4-phenyl-5-(4-(pyrrolidin-1-yl)benzoyl)thiazol-2-yl) cyclopropanecarboxamide ***(7n)***

Compound **7n** (11.5 mg, 21%) was prepared from (2-amino-4-phenylthiazol-5-yl) (4-(pyrrolidin-1-yl)phenyl) methanone (35 mg, 0.1 mmol) and benzo [1,3]dioxol-5-yl-cyclopropanecarboxylic acid (20.6 mg, 0.1 mmol) in the same manner as described for **7a** as pale yellow oil.

^{1}H NMR (200 MHz, DMSO-d_6): δ 12.08 (s, 1H, broad, NH); 7.82–6.75 (m, 12H, arom); 6.01 (s, 2H OCH_2O); 2.97 (m, 4H, $\underline{CH_2}N$); 1.88–1.43 (m, 6H, 4H CH_2CH_2, + 2H, CH_2, cyclopr); 1.40–1.12 (m, 2H, CH_2, cyclopr).

^{13}C NMR (50 MHz, DMSO-d_6): δ 187.7, 170.3, 160.2, 154.7, 146.9, 146.3, 131.8, 131.0, 129.6, 128.7, 128.2, 127.5, 123.3, 113.2, 110.2, 107.8, 100.6, 48.2, 30.3, 18.6, 15.4.

HRMS (ESI) calculated for $C_{31}H_{28}N_3O_4S$: $[M + H]^+$ 538.18004; found 538.17987.

4.1.15. N-(5-([1,1′-biphenyl]-3-carbonyl)-4-phenylthiazol-2-yl)-1-(benzo[d][1,3]dioxol-5-yl)cyc lopropanecarboxamide ***(7o)***

1-([1,1′-Biphenyl]-3-yl)ethanone (196 mg, 1 mmol) was brominated with *N*-bromosuccinimide (NBS) using the general procedure previously described [25] providing [1,1′-biphenyl]-3-carbonyl bromide intermediate (202 mg, 73%). The purity was verified by HPLC-MS without further purification.

A solution of [1,1′-biphenyl]-3-carbonyl bromide intermediate (130 mg, 0.5 mmol) and *N*-(bis(4-methoxybenzyl)carbamothioyl)-benzamide (230 mg, 0.5 mmol) in DMF (3 mL) was stirred at T = 85 °C for 3 h according to the protocol for compound **7a**. After TFA deprotection and crystallization in acetonitrile [1,1′-biphenyl]-3-yl (2-amino-4-phenylthiazol-5-yl)methanone (60,5 mg, 34%) was isolated. ESI-MS: *m*/*z* 357.1 $[M+H]^+$.

[1,1′-Biphenyl]-3-yl (2-amino-4-phenylthiazol-5-yl)methanone (36 mg, 0.1 mmol) and benzo [1,3] dioxol-5-yl-cyclopropanecarboxylic acid (20.6 mg, 0.1 mmol) was then conjugated in the same manner as described for **7a** to furnish, after HPLC purification, the title compound as pale yellow solid (12.5 mg, 23%).

^{1}H NMR (200 MHz, DMSO-d_6): δ 12.01 (s, 1H, broad, NH); 8.27–6.82 (m, 17H, arom); 6.04 (s, 2H OCH_2O); 1.69–1.42 (m, 2H, CH_2, cyclopr); 1.41–1.03 (m, 2H, CH_2, cyclopr).

^{13}C NMR (50 MHz, DMSO-d_6): δ 187.9, 171.8, 157.4, 153.3, 146.9, 146.3, 141.7, 137.8, 137.2, 131.3, 129.4, 128.8, 128.1, 127.5, 123.1, 110.2, 107.8, 100.6, 30.3, 15.6.

HRMS (ESI) calculated for $C_{33}H_{25}N_2O_4S$: $[M + H]^+$ 515.15349; found 545.15331.

4.1.16. 1-(Benzo[d][1,3]dioxol-5-yl)-N-(5-(2-methoxybenzoyl)-4-phenylthiazol-2-yl) cyclopropanecarboxamide ***(7p)***

Compound **7p** (11 mg, 22%) was prepared from (2-amino-4-phenylthiazol-5-yl) (2-methoxyphenyl) methanone (31 mg, 0.1 mmol) and benzo [1,3]dioxol-5-yl-cyclopropanecarboxylic acid (20.6 mg, 0.1 mmol) in the same manner as described for **7a** as brown oil.

^{1}H NMR (200 MHz, DMSO-d_6): δ 10.97 (s, 1H, broad, NH); 7.68–6.69 (m, 12H, arom); 6.02 (s, 2H OCH_2O); 3.98 (s, 3H, CH_3O); 1.68–1.43 (m, 2H, CH_2, cyclopr); 1.42–1.03 (m, 2H, CH_2, cyclopr).

^{13}C NMR (50 MHz, DMSO-d_6): δ 175.7, 163.1, 158.9, 154.4, 147.0, 146.3, 131.7, 131.1, 129.6, 128.9, 128.1, 127.5, 123.2, 113.8, 110.2, 107.8, 100.6, 97.7, 55.3, 30.3, 15.5.

HRMS (ESI) calculated for $C_{28}H_{23}N_2O_5S$: $[M + H]^+$ 499.13276; found 499.13276.

4.1.17. 1-(Benzo[d][1,3]dioxol-5-yl)-N-(5-(3-methoxybenzoyl)-4-phenylthiazol-2-yl) cyclopropanecarboxamide ***(7q)***

Compound **7q** (10.8 mg, 22%) was prepared from (2-amino-4-phenylthiazol-5-yl) (3-methoxyphenyl)methanone (31 mg, 0.1 mmol) and benzo [1,3]dioxol-5-yl-cyclopropanecarboxylic acid (20.6 mg, 0.1 mmol) in the same manner as described for **7a** as pale brown oil.

^{1}H NMR (200 MHz, DMSO-d_6): δ 12.04 (s, 1H, broad, NH); 7.94–6.76 (m, 12H, arom); 6.04 (s, 2H OCH_2O); 4.01 (s, 3H, CH_3O); 1.71–1.44 (m, 2H, CH_2, cyclopr); 1.40–1.02 (m, 2H, CH_2, cyclopr).

^{13}C NMR (50 MHz, DMSO-d_6): δ 177.4, 164.6, 158.4, 154.2, 146.9, 146.2, 131.8, 131.1, 129.7, 128.8, 128.1, 127.4, 123.2, 113.7, 110.2, 107.8, 100.6, 98.1, 55.6, 30.2, 15.4.

HRMS (ESI) calculated for $C_{28}H_{23}N_2O_5S$: $[M + H]^+$ 499.13276; found 499.13245.

4.1.18. 1-(Benzo[d][1, 3]dioxol-5-yl)-N-(5-(3-bromobenzoyl)-4-phenylthiazol-2-yl) cyclopropanecarboxamide ***(7r)***

Compound **7r** (16 mg, 29%) was prepared from (2-amino-4-phenylthiazol-5-yl) (3-bromophenyl)methanone (35.9 mg, 0.1 mmol) and benzo [1,3]dioxol-5-yl-cyclopropanecarboxylic acid (20.6 mg, 0.1 mmol) in the same manner as described for **7a** as pale brown solid.

^{1}H NMR (200 MHz, DMSO-d_6): δ 12.03 (s, 1H, broad, NH); 8.18–6.81 (m, 12H, arom); 6.06 (s, 2H OCH_2O); 1.78–1.45 (m, 2H, CH_2, cyclopr); 1.44–1.05 (m, 2H, CH_2, cyclopr).

^{13}C NMR (50 MHz, DMSO-d_6): δ 188.3, 172.1, 159.3, 155.3, 146.9, 146.3, 137.0, 131.2, 129.6, 129.0, 128.2, 127.5, 123.3, 114.2, 110.2, 107.8, 100.6, 30.3, 15.5.

HRMS (ESI) calculated for $C_{27}H_{20}BrN_2O_4S$: $[M + H]^+$ 547.03271; found 547.03219.

4.1.19. 1-(Benzo[d][1,3]dioxol-5-yl)-N-(5-(3-fluorobenzoyl)-4-phenylthiazol-2-yl) cyclopropanecarboxamide ***(7s)***

Compound **7s** (13 mg, 27%) was prepared from (2-amino-4-phenylthiazol-5-yl) (3-fluorophenyl)methanone (30 mg, 0.1 mmol) and benzo [1,3]dioxol-5-yl-cyclopropanecarboxylic acid (20.6 mg, 0.1 mmol) in the same manner as described for **7a** as white solid.

^{1}H NMR (200 MHz, DMSO-d_6): δ 11.93 (s, 1H, broad, NH); 8.01–6.74 (m, 12H, arom); 6.05 (s, 2H OCH_2O); 1.73–1.44 (m, 2H,

CH_2, cyclopr); 1.42−1.08 (m, 2H, CH_2, cyclopr).

^{13}C NMR (50 MHz, DMSO-d_6): δ 188.0, 171.5, 158.7, 156.2, 146.9, 146.3, 137.0, 133.4, 131.1, 129.7, 128.8, 128.2, 127.6, 123.2, 113.8, 110.2, 107.8, 100.6, 30.3, 15.5.

HRMS (ESI) calculated for $C_{27}H_{20}FN_2O_4S$: $[M + H]^+$ 487.11277; found 487.11243.

4.1.20. 1-(Benzo[d][1,3]dioxol-5-yl)-N-(5-(2,5-dimethoxybenzoyl)-4-phenylthiazol-2-yl) cyclopropanecarboxamide (7t)

Compound **7t** (13.8 mg, 26%) was prepared from (2-amino-4-phenylthiazol-5-yl) (2,5-dimethoxyphenyl)methanone (35 mg, 0.1 mmol) and benzo [1,3]dioxol-5-yl cyclopropanecarboxylic acid (20.6 mg, 0.1 mmol) in the same manner as described for **7a** as brown solid.

^{1}H NMR (200 MHz, DMSO-d_6) δ 11.85 (s, 1H, NH), 7.47−6.53 (m, 11H, arom); 6.02 (s, 2H, OCH_2O); 3.64 (s, 3H, OCH_3); 3.47 (s, 3H, OCH_3); 1.72−1.47 (m, 2H, CH_2, cyclopr); 1.37−1.16 (m, 2H, CH_2, cyclopr).

^{13}C NMR (50 MHz, DMSO-d_6) δ 172.3, 160.4, 155.2, 152.2, 149.9, 146.9, 146.3, 133.5, 131.7, 128.8, 128.1, 126.7, 123.3, 117.0, 113.5, 111.9, 110.3, 107.8, 100.6, 55.3, 55.2, 30.3, 15.5.

HRMS (ESI) calculated for $C_{29}H_{25}N_2O_6S$: $[M + H]^+$ 529.14332; found 529.14301.

4.1.21. 1-(Benzo[d][1,3]dioxol-5-yl)-N-(5-(2,4-dimethoxybenzoyl)-4-phenylthiazol-2-yl) cyclopropanecarboxamide (7u)

Compound **7u** (18.1 mg, 34%) was prepared from (2-amino-4-phenylthiazol-5-yl) (2,4-dimethoxyphenyl)methanone (34 mg, 0.1 mmol) and benzo [1,3]dioxol-5-yl-cyclopropanecarboxylic acid (20.6 mg, 0.1 mmol) in the same manner as described for **7a** as brown solid.

^{1}H NMR (200 MHz, DMSO-d_6) δ 11.98 (s, 1H, NH); 7.62−6.64 (m, 11H, arom); 6.04 (s, 2H, OCH_2O); 3.73 (s, 3H, OCH_3); 3.62 (s, 3H, OCH_3); 1.70−1.45 (m, 2H, CH_2, cyclopr); 1.39−1.09 (m, 2H, CH_2, cyclopr).

^{13}C NMR (50 MHz, DMSO-d_6) δ 176.4, 170.6, 160.2, 155.3, 152.2, 146.9, 146.3, 133.8, 131.4, 128.9, 128.2, 126.7, 123.2, 117.8, 113.6, 110.2, 107.8, 100.6, 55.4, 55.2, 30.3, 15.5.

HRMS (ESI) calculated for $C_{29}H_{25}N_2O_6S$: $[M + H]^+$ 529.14332; found 529.14298.

4.1.22. 1-(Benzo[d][1,3]dioxol-5-yl)-N-(5-(3-chloro-4-methoxybenzoyl)-4-phenylthiazol-2-yl) cyclopropanecarboxamide (7v)

Compound **7v** (14.5 mg, 27%) was prepared (2-amino-4-phenylthiazol-5-yl) (3-chloro-4-methoxyphenyl)methanone (40 mg, 0.1 mmol) and benzo [1,3]dioxol-5-yl-cyclopropanecarboxylic acid (20.6 mg, 0.1 mmol) in the same manner as described for **7a** as brown oil.

^{1}H NMR (200 MHz, DMSO-d_6) δ 12.14 (s, 1H, NH); 8.03−6.75 (m, 11H, arom); 6.06 (s, 2H, OCH_2O); 3.77 (s, 3H, OCH_3); 1.78−1.46 (m, 2H, CH_2, cyclopr); 1.42−1.10 (m, 2H, CH_2, cyclopr).

^{13}C NMR (50 MHz, DMSO-d_6) δ 184.5, 171.5, 162.2, 156.8, 153.1, 146.8, 146.3, 140.5, 137.2, 131.2, 128.8, 128.2, 123.3, 118.1, 113.6, 110.2, 107.7, 100.6, 55.3, 30.3, 15.6.

HRMS (ESI) calculated for $C_{28}H_{22}ClN_2O_5S$: $[M + H]^+$ 533.09379; found 533.09336.

4.1.23. N-(5-(3-allyl-4-hydroxybenzoyl)-4-phenylthiazol-2-yl)-1-(benzo[d][1,3]dioxol-5-yl) cyclopropanecarboxamide (7w)

Compound **7w** (10 mg, 19%) was prepared from (3-allyl-4-hydroxyphenyl) (2-amino-4-phenylthiazol-5-yl)methanone (34 mg, 0.1 mmol) and benzo [1,3]dioxol-5-yl-cyclopropanecarboxylic acid (20.6 mg, 0.1 mmol) in the same manner as described for **7a** as brown oil.

^{1}H NMR (200 MHz, DMSO-d_6) δ 12.02 (s, 1H, NH); 9.73 (s, 1H, OH); 7.88−6.72 (m, 11H, arom); 6.05 (s, 2H, OCH_2O); 5.95−5.61 (m, 1H, $CH_2\underline{CH}{=}CH_2$); 4.92−4.68 (m, 2H, $CH_2CH{=}\underline{CH_2}$); 3.18 (d, J = 15.2, 2H, $\underline{CH_2}CH{=}CH_2$); 1.77−1.43 (m, 2H, CH_2, cyclopr); 1.42−1.14 (m, 2H, CH_2, cyclopr).

^{13}C NMR (50 MHz, DMSO-d_6) δ 178.4, 170.5, 161.1, 156.2, 152.9, 146.9, 146.3, 145.2, 136.9, 136.5, 131.2, 128.8, 128.3, 123.4, 114.2, 110.2, 107.8, 100.6, 34.9, 30.3, 15.6.

HRMS (ESI) calculated for $C_{30}H_{25}N_2O_5S$: $[M + H]^+$ 525.14841; found 525.14803.

4.1.24. 5-(2-(1-(Benzo[d][1,3]dioxol-5-yl) cyclopropanecarboxamido)-4-phenylthiazole-5-carbonyl)-2-hydroxybenzamide (7x)

Compound **7x** (12.5 mg, 24%) was prepared from 5-(2-amino-4-phenylthiazole-5-carbonyl)-2-hydroxybenzamide (34 mg, 0.1 mmol) and benzo [1,3]dioxol-5-yl-cyclopropanecarboxylic acid (20.6 mg, 0.1 mmol) in the same manner as described for **7a** as brown oil.

^{1}H NMR (200 MHz, DMSO-d_6) δ 11.89 (s, 1H, NH); 11.38 (s, 1H, OH); 8.55 (s, 2H, NH_2); 7.64−6.68 (m, 11H, arom); 6.05 (s, 2H, OCH_2O); 1.72−1.42 (m, 2H, CH_2, cyclopr); 1.42−1.05 (m, 2H, CH_2, cyclopr).

^{13}C NMR (50 MHz, DMSO-d_6) δ 180.4, 172.6, 168.3, 159.7, 155.5, 152.8, 146.9, 146.3, 137.1, 131.3, 128.9, 128.2, 126.7, 123.4, 113.9, 110.2, 107.7, 100.6, 30.3, 15.5.

HRMS (ESI) calculated for $C_{28}H_{22}N_3O_6S$: $[M + H]^+$ 528.12292; found 528.12282.

4.1.25. 1-(Benzo[d][1,3]dioxol-5-yl)-N-(5-(5-chloro-2-hydroxybenzoyl)-4-phenylthiazol-2-yl) cyclopropanecarboxamide (7y)

Compound **7y** (11.2 mg, 11%) was prepared from (2-amino-4-phenylthiazol-5-yl) (5-chloro-2-hydroxyphenyl)methanone (66 mg, 0.19 mmol) and benzo [1,3]dioxol-5-yl-cyclopropanecarboxylic acid (39 mg, 0.19 mmol) in the same manner as described for **7a** as brown oil.

^{1}H NMR (200 MHz, DMSO-d_6) δ 12.06 (s, 1H, NH); 10.84 (s, 1H, OH); 8.01−6.71 (m, 11H, arom); 6.05 (s, 2H, OCH_2O); 1.73−1.45 (m, 2H, CH_2, cyclopr); 1.43−1.05 (m, 2H, CH_2, cyclopr).

^{13}C NMR (50 MHz, DMSO-d_6) δ 185.6, 172.7, 160.9, 155.9, 153.3, 146.9, 146.2, 141.8, 137.3, 131.1, 128.9, 128.1, 123.2, 117.5, 113.8, 110.2, 107.7, 100.6, 30.3, 15.5.

HRMS (ESI) calculated for $C_{27}H_{20}ClN_2O_5S$: $[M + H]^+$ 519.07814; found 599.07781.

4.1.26. 1-(Benzo[d][1,3dioxol-5-yl)-N-(5-(benzo[d][1, 3]dioxole-5-carbonyl)-4-phenylthiazol-2-yl) cyclopropanecarboxamide (7z)

Compound **7z** (15.5 mg, 30%) was prepared from (2-amino-4-phenylthiazol-5-yl) (benzo [d] [1,3] dioxol-5-yl)methanone (32.4 mg, 0.1 mmol) and benzo [1,3]dioxol-5-yl-cyclopropanecarboxylic acid (20.6 mg, 0.1 mmol) in the same manner as described for **7a** as brown oil.

^{1}H NMR (200 MHz, DMSO-d_6) δ 12.08 (s, 1H, NH); 7.77−6.68 (m, 11H, arom); 6.07 (s, 2H, OCH_2O); 6.03 (s, 2H, OCH_2O); 1.64−1.41 (m, 2H, CH_2, cyclopr); 1.41−1.00 (m, 2H, CH_2, cyclopr).

^{13}C NMR (50 MHz, DMSO-d_6) δ 178.8, 171.4, 159.3, 154.8, 151.5, 146.9, 146.3, 137.0, 131.2, 128.8, 128.1, 127.4, 123.2, 114.6, 110.3, 107.8, 100.6, 30.3, 15.4.

HRMS (ESI) calculated for $C_{28}H_{21}N_2O_6S$: $[M + H]^+$ 513.11203; found 513.11187.

4.1.27. 2-(1-(Benzo[d][1,3]dioxol-5-yl)cyclopropanecarboxamido)-N,4-diphenylthiazole-5-carboxamide (12a)

A solution of ethyl 2-amino-4-phenylthiazole-5-carboxylate

(248 mg, 1 mmol), di-*tert*-butyl carbonate (262 mg, 1.2 mmol) and catalytic 4-(*N*,*N*-dimethylamino) pyridine (8 mg, 0.07 mmol) in anhydrous THF (1 mL) was stirred for 4 h at room temperature. The mixture was concentrated under vacuum and after extraction with EtOAc (3 x 3 mL), washed with H_2O (3 x 2 mL). The organic phases were dried over Na_2SO_4, and concentrated under vacuum. Crystallization in acetonitrile afford ethyl 2-((*tert*-butoxycarbonyl) amino)-4-phenylthiazole-5-carboxylate (170 mg, 49%) which was used in the next step without further purification. ESI-MS: *m*/*z* 349.1 $[M+H]^+$.

A solution of ethyl 2-((*tert*-butoxycarbonyl)amino)-4-phenylthiazole-5-carboxylate (170 mg, 0.49 mmol) in THF-EtOH (2.5 mL, 1:1.5) and 6 N aq KOH solution (1 mL) was heated at T = 55 °C for 4 h. The solution was cooled to T = 0 °C and acidified with conc. HCl to pH 1. The solution was then concentrated in vacuum, and after extraction with diethyl ether (3 x 3 mL), washed with H_2O (3 x 2 mL) and dried over anhydrous Na_2SO_4. After filtration, the solution was evaporated to obtain 2-[[(tert-butyloxy) carbonyl]-amino]-4-phenyl-1,3-thiazole-5-carboxylic acid (100 mg, 64%) as a brown solid. ESI-MS: *m*/*z* 321.1 $[M+H]^+$.

The 2-[[(tert-butyloxy)carbonyl]-amino]-4-phenyl-1,3-thiazole-5-carboxylic acid (75 mg, 0.23 mmol) was resuspended in anhydrous DMF (1 mL), HATU (87 mg, 0.23 mmol) and DIPEA (40 μL, 0.23 mmol) were added. The reaction was vigorously stirred for 5 min and aniline (23 μL, 0.24 mmol) in anhydrous DMF (500 μL) was added. The reaction was kept at T = 40 °C for 2 h. Solvent was removed under reduced pressure and the residue was partitioned between diethyl ether and water. The combined organic layers were washed with water (3 x 2 mL), and then dried over anhydrous Na_2SO_4. After filtration, solvent was removed in vacuum and the residue was stirred in a mixture of TFA: DCM 1:1 (2 mL) at T = 0 °C until complete deprotection (4–5 h). Most of TFA was removed under reduced pressure. The residue was neutralized with $NaHCO_3$ 1 N and then extracted with EtOAc for 3 times. Crystallization in acetonitrile furnishes 2-amino-N,4-diphenylthiazole-5-carboxamide (30 mg, 44%). ESI-MS: *m*/*z* 296.1 $[M+H]^+$.

Benzo [1,3]dioxol-5-yl-cyclopropanecarboxylic acid (20.5 mg, 0.1 mmol) was resuspended in anhydrous DMF (1 mL); HATU (38 mg, 0.1 mmol) and DIPEA (18 μL, 0.1 mmol) were added. After 5 min, 2-amino-N, 4-diphenylthiazole-5-carboxamide (30 mg, 0.1 mmol) in anhydrous DMF (500 μL) was added. The reaction was kept at T = 50 °C until completeness (about 24 h).

The mixture was concentrated under vacuum and after extraction with EtOAc (3 x 3 mL), washed with H_2O (3 x 2 mL). The organic phase was dried over Na_2SO_4, concentrated under reduced pressure and purified by preparative HPLC. The peak of interest was concentrated to obtain the title compound as white solid with purity of >95% as determined by HPLC-MS (10 mg, 21%).

^{1}H NMR (200 MHz, DMSO-d_6): δ 12.08 (s, broad, 1H, NH); 10.63 (s, broad, 1H, NH); 7.79–6.75 (m, 13H, arom); 6.05 (s, 2H OCH_2O); 1.81–1.45 (m, 2H, CH_2, cyclopr); 1.43–1.01 (m, 2H, CH_2, cyclopr).

^{13}C NMR (50 MHz, DMSO-d_6) δ 183.5, 165.5, 161.9, 151.0, 146.8, 146.3, 137.9, 137.0, 129.2, 128.9, 128.7, 128.0, 127.5, 121.6, 116.0, 110.8, 107.2, 101.2, 30.3, 15.6.

HRMS (ESI) calculated for $C_{27}H_{22}N_3O_4S$: $[M + H]^+$ 484.13309; found 484.13277.

4.1.28. N-(2-(1-(Benzo[d][1,3]dioxol-5-yl) cyclopropanecarboxamido)-4-(4-methoxyphenyl)thiazol-5-yl) benzamide **(12b)**

To a stirred solution of 4-methoxyphenacyl bromide (229 mg, 1 mmol) in diethyl ether (2 mL) was added hexamethylenetetramine (140 mg, 1 mmol) all at once and the mixture was stirred for 2 h at room temperature. The resulting solid was centrifugated, washed with diethyl ether (2 mL), and dried under reduced pressure to afford the quaternary salt. To the compound, EtOH (2 mL) and conc. HCl (0.1 mL) were added and the mixture was refluxed for 3 h. After cooling to room temperature, the solid was centrifugated, washed with EtOH (3 x 2 mL), and dried under vacuum to afford pure 4-methoxy2′amino-acetophenone hydrochloride in near quantitative yield. ESI-MS: *m*/*z* 202.6 $[M+H]^+$.

$NaHCO_3$ (252 mg, 3 mmol) was added to a solution of 4-methoxy2′amino-acetophenone hydrochloride (202 mg, 1 mmol) in anhydrous THF (2 mL) with stirring at room temperature. Benzoyl chloride (116 μl, 1 mmol) was added to the solution and stirred for about 3 h at room temperature. The solvent was removed under reduced pressure to leave a yellow oil. The product was extracted with dichloromethane (DCM) (3 x 3 mL) and washed with H_2O (3 x 2 mL). The organic phase was dried over Na_2SO_4 and then concentrated under reduced pressure. Removal of the solvent produced the *N*-(2-(4-methoxyphenyl)-2-oxoethyl)benzamide as a white solid of sufficient purity to be used in the next step (202 mg, 75%). ESI-MS: *m*/*z* 269.1 $[M+H]^+$.

N-(2-(4-methoxyphenyl)-2-oxoethyl)benzamide (107 mg, 0.4 mmol) and thiourea (30 mg, 0.4 mmol) were solved in EtOH at room temperature. To this solution I_2 (101 mg, 0.4 mmol) and triethylamine (TEA) (11 μl, 0.2 mmol) were added. The reactions were stirred at T = 80 °C overnight. The mixture was concentrated under vacuum and after extraction with EtOAc (3 x 3 mL), was washed with H_2O (3 x 2 mL). The organic layer was dried over anhydrous Na_2SO_4. After filtration, solvent was removed in vacuum to obtain *N*-(2-amino-4-(4-methoxyphenyl)thiazol-5-yl) benzamide (40 mg, 31%). The thiazole was used without further purification. ESI-MS: *m*/*z* 325.1 $[M+H]^+$.

Benzo [1,3]dioxol-5-yl-cyclopropanecarboxylic acid (25 mg, 0.12 mmol) was resuspended in anhydrous DMF (1 mL), HATU (45 mg, 0.12 mmol) and DIPEA (42 μL, 0.24 mmol) were added. After 5 min, *N*-(2-amino-4-(4-methoxyphenyl)thiazol-5-yl)benzamide (40 mg, 0.12 mmol) in anhydrous DMF (500 μL) was added. The reaction was kept at T = 50 °C until completeness (about 24 h).

The mixture was concentrated under vacuum and after extraction with EtOAc (3 x 3 mL), washed with H_2O (3 x 2 mL). The organic phase was dried over Na_2SO_4, concentrated under reduced pressure and purified by preparative HPLC. The peak of interest was concentrated to obtain the title compound as brown solid with purity of >95% as determined by HPLC-MS (11 mg, 18%).

^{1}H NMR (200 MHz, DMSO-d_6): δ 12.19 (s, broad, 1H, NH); 11.59 (s, broad, 1H, NH); 8.02–6.81 (m, 12H, arom); 6.04 (s, 2H OCH_2O); 3.86 (s, 3H, OCH_3); 1.78–1.44 (m, 2H, CH_2, cyclopr); 1.41–1.08 (m, 2H, CH_2, cyclopr).

^{13}C NMR (50 MHz, DMSO-d_6) δ 180.8, 167.3, 160.5, 151.4, 146.9, 146.4, 137.8, 136.8, 129.2, 128.9, 128.1, 127.5, 121.7, 116.3, 110.8, 107.2, 101.2, 53.7, 30.3, 15.5.

HRMS (ESI) calculated for $C_{28}H_{24}N_3O_5S$: $[M + H]^+$ 514.14366; found 514.14359.

4.1.29. 1-(Benzo[d][1,3]dioxol-5-yl)-N-(5-(4-methylbenzoyl) thiazol-2-yl)cyclopropanecarboxamide **(12c)**

N,*N*-Dimethyl formamide dimethyl acetal (1036 μL, 7.8 mmol) was added to a suspension of thiourea (198 mg, 2.6 mmol) in DCM (2 mL). The mixture was heated at reflux for 4 h. The solvent was removed and the residue was crystallized from diethyl ether to obtain (1E, 1′E)-N′,N″-thiocarbonylbis (*N*,*N*-dimethylformimidamide) (400 mg, 83%). ESI-MS: *m*/*z* 187.1 (M + H) +.

(1E, 1′E)-*N*′,*N*″-Thiocarbonylbis-(*N*,*N*-dimethylformimidamide (100 mg, 0.53 mmol) was suspended in THF (1 mL) and 2-bromo4′-methylacetophenone (113 mg, 0.53 mmol) was added. The mixture was stirred at room temperature for 15 min and then TEA (147 μL, 1.16 mmol) was added and the mixture was heated at reflux for 18 h. The mixture was concentrated under vacuum and after

extraction with EtOAc (3 x 3 mL), washed with H_2O (3 x 2 mL). The organic phase was dried over Na_2SO_4, concentrated under reduced pressure to obtain (Z)-*N*'-(5-(4-methylbenzoyl) thiazol-2-yl)-*N*,*N*-dimethylformimidamide (108 mg, 70%). ESI-MS: *m*/*z* 273.1 (M + H) +.

A 33% (wt./wt.) aqueous methylamine (400 μL) was added to a solution of (Z)-*N*'-(5-(4-methylbenzoyl)thiazol-2-yl)-*N*,*N*-dimethylformimidamide (101 mg, 0,37 mmol) in THF (1 mL) and the mixture was stirred for 24 h at room temperature. The mixture was concentrated under vacuum and after extraction with EtOAc (3 x 3 mL), washed with H_2O (3 x 2 mL). The organic phase was dried over Na_2SO_4, concentrated under reduced pressure to obtain a pale yellow oil. Crystallization in acetonitrile furnishes (2-aminothiazol-5-yl) (*p*-tolyl)methanone (36 mg, 45%). ESI-MS: *m*/*z* 219.1 $[M+H]^+$.

Benzo [1,3]dioxol-5-yl-cyclopropanecarboxylic acid (33 mg, 0.16 mmol) was resuspended in anhydrous DMF (1 mL), HATU (61 mg, 0.16 mmol) and DIPEA (56 μL, 0.16 mmol) were added. After 5 min, (2-aminothiazol-5-yl) (*p*-tolyl) methanone (35 mg, 0.16 mmol) in anhydrous DMF (500 μL) was added. The reaction was kept at T = 50 °C until completeness (about 24 h).

The mixture was concentrated under vacuum and after extraction with EtOAc (3 x 3 mL), washed with H_2O (3 x 2 mL). The organic phase was dried over Na_2SO_4, concentrated under reduced pressure and purified by preparative HPLC. The peak of interest was concentrated to obtain the title compound as pale yellow solid with purity of >95% as determined by HPLC-MS (32.4 mg, 50%).

^{1}H NMR (200 MHz, DMSO-d_6): δ 11.87 (s, broad, 1H, NH); 8.05 (s, 1H, arom); 7.81–6.78 (m, 7H, arom); 6.04 (s, 2H OCH_2O); 2.32 (s, 3H, CH_3); 1.81–1.42 (m, 2H, CH_2, cyclopr); 1.41–1.00 (m, 2H, CH_2, cyclopr).

^{13}C NMR (50 MHz, DMSO-d_6) δ 186.2, 173.6, 146.8, 146.3, 137.0, 133.1, 129.6, 129.1, 121.3, 110.8, 107.2, 101.2, 30.3, 24.6, 15.5.

HRMS (ESI) calculated for $C_{22}H_{19}N_2O_4S$: $[M + H]^+$ 407.10654; found 407.10608.

4.1.30. 1-(Benzo[d][1,3]dioxol-5-yl)-N-(5-(4-methoxybenzoyl) thiazol-2-yl)cyclopropanecarboxamide ***(12d)***

(1E, 1′E)-N′,N″-Thiocarbonylbis-*N*,*N*-dimethylformimidamide (100 mg, 0.53 mmol) was suspended in DCM (1 mL) and 2-bromo-4′-methoxyacetophenone (121 mg, 0.53 mmol) was added. The mixture was stirred at room temperature for 15 min and then TEA (147 μL, 1.16 mmol) was added. The mixture was heated at reflux for about 20 h. At the end of the reaction the solution was concentrated under vacuum and after extraction with EtOAc (3 x 3 mL), washed with H_2O (3 x 2 mL). The organic phase was dried over Na_2SO_4, concentrated under reduced pressure to obtain (Z)-*N*'-(5-(4-methoxybenzoyl) thiazol-2-yl)-*N*,*N*-dimethylformimidamide (108 mg, 70%).

ESI-MS: *m*/*z* 290.1 $[M+H]^+$.

A 33% (wt./wt.) aqueous methylamine (600 μL) was added to a solution of (Z)-*N*'-(5-(4-methoxybenzoyl)thiazol-2-yl)-*N*,*N*-dimethylformimidamide (108 mg, 0.37 mmol) in THF (1 mL) and the mixture was stirred for 24 h at room temperature. The solution was then concentrated under vacuum and after extraction with EtOAc (3 x 3 mL), washed with H_2O (3 x 2 mL). The organic phase was dried over Na_2SO_4, concentrated under reduced pressure to obtain a yellow oil. Crystallization in acetonitrile furnishes (2-aminothiazol-5-yl) (4-methoxyphenyl)methanone (46 mg, 53%). MS ESI-MS: *m*/*z* 235.1 $[M+H]^+$.

Benzo [1,3]dioxol-5-yl-cyclopropanecarboxylic acid (39 mg, 0.19 mmol) was resuspended in anhydrous DMF (1 mL), HATU (72 mg, 0.19 mmol) and DIPEA (66 μL, 0.19 mmol) were added. After 5 min, (2-aminothiazol-5-yl) (4-methoxyphenyl)methanone (45 mg, 0.19 mmol) in anhydrous DMF (500 mL) was added. The reaction was kept at T = 50 °C until completeness (about 36 h).

The mixture was concentrated under vacuum and after extraction with EtOAc (3 x 3 mL), washed with H_2O (3 x 2 mL). The organic phase was dried over Na_2SO_4, concentrated under reduced pressure and purified by preparative HPLC. The peak of interest was concentrated to obtain the title compound as brown solid with purity of >95% as determined by HPLC-MS (26.6 mg, 33%).

^{1}H NMR (200 MHz, DMSO-d_6): δ 11.87 (s, broad, 1H, NH); 8.08 (s, 1H, arom); 7.79–6.81 (m, 7H, arom); 6.04 (s, 2H OCH_2O); 3.89 (s, 3H, CH_3); 1.78–1.41 (m, 2H, CH_2, cyclopr); 1.40–1.03 (m, 2H, CH_2, cyclopr).

^{13}C NMR (50 MHz, DMSO-d_6) δ 182.7, 171.9, 146.9, 146.3, 137.1, 133.0, 129.7, 128.8, 121.4, 110.8, 107.2, 101.2, 55.9, 30.3, 15.5.

HRMS (ESI) calculated for $C_{22}H_{19}N_2O_5S$: $[M + H]^+$ 423.10146; found 423.10098.

4.1.31. N-(5-Acetyl-4-phenylthiazol-2-yl)-1-(benzo[d][1,3]dioxol-5-yl)cyclopropanecarboxamide ***(24a)***

Compound **24a** (9.6 mg, 24%) was prepared from 1-(2-amino-4-phenylthiazol-5-yl) ethanone (22.1 mg, 0.1 mmol) and benzo [1,3] dioxol-5-yl-cyclopropanecarboxylic acid (20.6 mg, 0.1 mmol) in the same manner as described for **7a** until completeness (18 h) as white solid.

^{1}H NMR (200 MHz, DMSO-d_6): δ 11.94 (s, broad, 1H, NH); 7.64–6.59 (m, 8H, arom); 6.02 (s, 2H OCH_2O); 2.62 (s, 3H, CH_3); 1.74–1.43 (m, 2H, CH_2, cyclopr); 1.40–1.16 (m, 2H, CH_2, cyclopr).

^{13}C NMR (50 MHz, DMSO-d_6) δ 192.5, 180.4, 164.2, 151.0, 146.8, 146.3, 137.0, 131.9, 129.2, 128.7, 127.5, 116.0, 110.2, 107.6, 101.2, 30.3, 29.7, 15.6.

HRMS (ESI) calculated for $C_{22}H_{19}N_2O_4S$: $[M + H]^+$ 407.10655; found 407.10611.

4.1.32. 1-(Benzo[d][1,3]dioxol-5-yl)-N-(5-nicotinoyl-4-phenylthiazol-2 yl)cyclopropanecarboxamide ***(24 b)***

Compound **24b** (16 mg, 34%) was prepared from (2-amino-4-phenylthiazol-5-yl) (pyridin-3-yl)methanone (28 mg, 0.1 mmol) and benzo [1,3]dioxol-5-yl-cyclopropanecarboxylic acid (20.6 mg, 0.1 mmol) in the same manner as described for **7a** until completeness (24 h) as brown oil.

^{1}H NMR (200 MHz, DMSO-d_6): δ 12.04 (s, broad, 1H, NH); 8.62–8.22 (m, 3H, arom); 7.93–6.76 (m, 9H, arom); 6.06 (s, 2H OCH_2O); 1.73–1.41 (m, 2H, CH_2, cyclopr); 1.37–1.02 (m, 2H, CH_2, cyclopr).

^{13}C NMR (50 MHz, DMSO-d_6) δ 178.8, 171.5, 164.3, 155.0, 151.7, 146.9, 146.3, 141.8, 138.3, 136.9, 133.2, 129.2, 128.7, 127.5, 124.4, 116.0, 111.8, 107.8, 101.2, 30.3, 15.5.

HRMS (ESI) calculated for $C_{26}H_{20}N_3O_4S$: $[M + H]^+$ 470.11745; found 470.11708.

4.1.33. 1-(Benzo[d][1,3]dioxol-5-yl)-N-(5-(morpholine-4-carbonyl)-4-phenylthiazol-2-yl)cyclopropanecarboxamide ***(24c)***

Compound **24c** (12.8 mg, 27%) was prepared from (2-amino-4-phenylthiazol-5-yl) (morpholino)methanone (29 mg, 0.1 mmol) and benzo [1,3]dioxol-5-yl-cyclopropanecarboxylic acid (20.6 mg, 0.1 mmol) in the same manner as described for **7a** until completeness (24 h) as yellow solid.

^{1}H NMR (200 MHz, DMSO-d_6): δ 11.91 (s, broad, 1H, NH); 7.72–6.58 (m, 8H, arom); 6.03 (s, 2H OCH_2O); 3.72 (t, J = 6.8, 4H, OCH_2); 2.67 (t, J = 6.8, 4H, NCH_2); 1.78–1.43 (m, 2H, CH_2, cyclopr); 1.41–1.06 (m, 2H, CH_2, cyclopr).

^{13}C NMR (50 MHz, DMSO-d_6) δ 176.3, 169.8, 162.5, 151.2, 146.9, 146.4, 137.0, 131.1, 129.2, 128.7, 127.5, 116.0, 110.8, 10.2, 101.2, 56.2, 42.8, 30.3, 15.6.

HRMS (ESI) calculated for $C_{25}H_{24}N_3O_5S$: $[M + H]^+$ 478.14366; found 478.14327.

4.2. Molecular modeling

All the compounds were built, parameterized (Gasteiger-Huckel method) and energy minimized within MOE using MMFF94 forcefield [MOE: Chemical Computing Group Inc. Montreal. H3A 2R7 Canada. http://www.chemcomp.com]. Docking calculations were performed taking into account the X-ray structure of the F508del-CFTR *h*NBD1 domain (pdb code = 4WZ6, resolution = 2.05 Å) [41] by means of LeadIT 2.1.8 software suite (www.biosolveit.com). In particular, molecular docking studies of the explored hybrids and reference correctors VX-809, ALK-809 and SUL-809 were performed considering the putative binding site within the NBD1 domain as proposed by the site finder module of MOE software. Then, docking calculations were performed by means of LeadIT 2.1.8 software suite (www.biosolveit.com) starting from the best scored *h*NBD1-VX-809 complex previously derived by automatic docking with MOE software. The final docking poses were prioritized by the score values of the lowest energy pose of the compounds docked to the protein structure. All ligands were refined and rescored by assessment with the algorithm HYDE, included in the LeadIT 2.1.8 software. The HYDE module considers dehydration enthalpy and hydrogen bonding [42,43].

4.3. Biological evaluations

4.3.1. Cell culture

The bronchial epithelial cell line CFBE41o-with stable co-expression of F508del-CFTR and the halide-sensitive yellow fluorescent protein (HS-YFP) was cultured with MEM medium supplemented with 10% fetal calf serum, 2 mM L-glutamine, 100 U/mL penicillin, and 100 mg/mL streptomycin.

4.3.2. Fluorescence assay for CFTR activity

CFBE41o-cells with expression of mutant CFTR and HS-YFP were plated on clear-bottom 96-well black microplates (Corning Life Sciences, Acton, MA) at a density of 50,000 cells/well and kept at.

37 °C in 5% CO_2 for 24 h. For the corrector assay, CFBE41o-cells were treated for further 24 h with compounds and/or VX-809 or VX-661. After treatment, the culture medium was removed and cells in each well were stimulated for 30 min at 37 °C with 60 mL PBS (containing 137 mM NaCl, 2.7 mM KCl, 8.1 mM Na_2HPO_4, 1.5 mM KH_2PO_4, 1 mM $CaCl_2$, and 0.5 mM $MgCl_2$) plus forskolin (20 μM) and genistein (50 μM).

At the time of assay, microplates carrying CFBE41o-cells were transferred to a microplate's reader (FluoStar Galaxy; BMG Labtech, Offenburg, Germany). The plate reader was equipped with high quality excitation (HQ500/20X: 500 ± 10 nm) and emission (HQ535/30 M: 535 ± 15 nm) filters for YFP (Chroma Technology, Brattleboro, VT). The assay consisted of a continuous 14 s fluorescence reading with 2 s before and 12 s after injection of an iodide containing solution (165 mL of a modified PBS containing I- instead of Cl-; final I- concentration in the well: 100 mM). Data were normalized to the initial background-subtracted fluorescence. To determine fluorescence quenching rate associated with I- influx, the final 10 s of data for each well were fitted with an exponential function to extrapolate initial slope (dF/dt).

Dose-response relationships from each experiment were fitted with the Hill equation using the Igor software (WaveMetrics) to calculate EC_{50}, maximal effect, and Hill coefficient.

4.3.3. Transepithelial electrical resistance (TEER) evaluation

Primary bronchial epithelial cells obtained from one patient with CF (homozygous for F508del mutation) were seeded at high density on porous membranes (200.000 cells for 0.33-cm^2 mini-Transwell inserts (Corning, code 3379) for transepithelial electrical resistance (TEER). To test putative correctors, compounds were added to the basolateral medium for 24 h at 37 °C and 5% CO_2, before measuring the TEER. Control epithelia were treated with vehicle alone (DMSO). TEER was measured in each well under basal conditions, after ENaC inhibition with apical amiloride (10 μM), after CFTR stimulation with forskolin (10 μM) and genistein (50 μM) on both sides, and after CFTR inhibition with apical PPQ102 (30 μM). After each treatment, we waited 10 min before recording electrical parameters. The TEER values for each well were converted into short-circuit current equivalent by Ohm's law. The TEER values were converted into TEEC.

4.3.4. Biochemical analysis of CFTR expression pattern

CFBE41o-cells stably expressing mutant CFTR and HS-YFP were grown to confluence on 60-mm diameter dishes and treated for 24 h with test compounds or vehicle alone. After 24 h cells were lysed in RIPA buffer containing a complete protease inhibitor (Roche). Cell lysates were subjected to centrifugation at 12000 rpm at 4 °C for 10min. Supernatant protein concentration was calculated using the BCA assay (Euroclone) following the manufacturer's instructions. Equal amounts of protein (10 μg) were separated onto gradient (4–15%) Criterion TGX Precast gels (Bio-rad laboratories Inc.), transferred to nitrocellulose membrane with *Trans*-Blot Turbo system (Bio-rad Laboratories Inc.) and analyzed by Western blotting. Proteins were detected using monoclonal anti-

CFTR (596, Cystic Fibrosis Foundation Therapeutics, University of North Carolina, Chapel Hill) or mouse monoclonal *anti*-GAPDH (cl.6C5; Santa Cruz Biotechnology, Inc) followed by horseradish peroxidase (HRP)-conjugated anti-mouse IgG (Abcam), and subsequently visualized by chemiluminescence using the SuperSignal West Femto Substrate (Thermo Scientific). Chemiluminescence was monitored using the Molecular Imager ChemiDoc XRS System. Images were analyzed with ImageJ software (National Institutes of Health). Bands were analyzed as ROI, normalized against the GAPDH loading control. Data are presented as mean ± SEM of independent experiments.

4.3.5. Statistics

Each experimental condition was tested in three independent experiments, each one performed with three biological replicates (n = 9). The Kolmogorov–Smirnov test was used to evaluate the assumption of normality. Statistical significance of the effect of single treatments on CFTR activity or expression was tested by parametric 1-way ANOVA followed by the Dunnet multiple comparisons test (all groups against the control group) as post-hoc test. In the case of combination of treatments, statistical significance was verified by ANOVA followed by the Tukey test (for multiple comparisons) as post-hoc test. Normally distributed data are expressed as mean ± SD or mean ± SEM, as indicated, and significances are two-sided. Differences were considered statistically significant when P was less than 0.05.

4.4. Surface plasmon resonance binding assays

His-tagged human intact F508del-CFTR protein purified as described [44,45] was provided by Prof. R.C. Ford, Manchester University, UK. Lipids [synthetic phospholipid blend (Dioleoyl) DOPC: DOPS [(7:3 w/w)] were from Avant Polar Lipids (Alabaster, AL). CHAPS and cholesteryl hemi succinate (CHS) Tris salt were from Sigma-Aldrich (St Louis, MO). Carboxy-methyl dextran CM5 sensor chip, anti-His antibody, 1-ethyl-3-(3-diaminopropyl)-carbodiimide hydrochloride (EDC) and *N*-hydroxysuccinimide (NHS) were from GE-Healthcare (Milwaukee, WI).

A BIAcore X-100 instrument (GE-Healthcare) was used. The preparation of the biosensor containing F508del-CFTR in a

membrane-like lipid environment was prepared as described [38]. Briefly, anti-His antibody was immobilized on a CM5 sensor chip by standard amine-coupling chemistry. After sensor chip equilibration by injection of DOPC:DOPS (7:3 W/W) 0.075 μg/mL, 0.02% CHS, 0.1% CHAPS (DOPC:DOPS running buffer), human His-tagged intact F508del-CFTR (10 μg/mL, Hepes 50 mM, pH 7 containing NaCl 150 mM DOPC: DOPS (7:3 W/W) 363 μg/mL, 0.06% CHS, 0.3% CHAPS (DOPC:DOPS-F508del-CFTR buffer), was injected on the anti-His surface, allowing the capture of about 1125 RU. A sensor chip coated with anti-His antibody alone was used for blank subtraction.

To evaluate their F508del-CFTR-binding capacity, compounds were injected over the sensor chip at increasing concentration in PBS, 0.05% surfactant P20 and 5% DMSO, pH 7.4 (PBS-DMSO) by adopting the single cycle model [46]. Dissociation Constant (Kd) values were calculated by steady state analyses performed by fitting the proper form of Scatchard's equation for the plot of the bound resonance units (RU) at equilibrium versus the compound concentration in solution.

Author contributions

The manuscript was written through contributions of all authors. All authors have given approval to the final version of the manuscript.

AP and GR performed synthesis and HPLC purification of the new compounds, EP and VT performed biological studies, BT determined and interpreted NMR spectra. AS and GD performed mass spectrometry characterization of all compounds. CU prepared SPR biosensors and performed SPR analysis. MR interpreted SPR results. NP performed biological studies and contributed analytical tools. EC conceived, performed and interpreted all computational studies. EM conceived the compounds, designed, coordinated and supervised the whole project. EC, MR and NP contributed to write the manuscript. EM critically revised the entire manuscript.

Notes

The authors declare no competing financial interest.

Declaration of competing interest

The authors declare that they have no known competing financial interests or personal relationships that could have appeared to influence the work reported in this paper.

Acknowledgment

We wish to thank Prof. Robert C. Ford, University of Manchester, UK for providing purified intact human F508del-CFTR protein.

This work was supported by Fondazione Italiana Fibrosi Cistica FFC#6/2017 to EM and EC (with the contribution of Delegazione FFC di Verona Valpolicella), FFC #10/2019 to MR (with the contribution of Delegation of Vittoria Ragusa, Siracusa e Catania Mascalucia) and FFC #9/2019 to NP (with the contribution of "Delegazione FFC di Genova con Gruppo di sostegno FFC di Savona Spotorno", "Delegazione FFC di Valle Scrivia Alessandria", "Delegazione FFC di Montescaglioso", and "Delegazione FFC di Ascoli Piceno"). Work in NP lab is also supported by the Italian Ministry of Health through Cinque per Mille and Ricerca Corrente (Linea 1).

Appendix A. Supplementary data

Supplementary data to this article can be found online at https://doi.org/10.1016/j.ejmech.2020.112833.

References

[1] J.R. Riordan, J.M. Rommens, B. Kerem, N. Alon, R. Rozmahel, Z. Grzelczak, J. Zielenski, S. Lok, N. Plavsic, J.L. Chou, M.L. Drumm, M.C. Iannuzzi, F.S. Collins, L.-C. Tsui, Identification of the cystic fibrosis gene: Cloning and characterization of complementary DNA, Science 245 (4922) (1989) 1066–1073.

[2] D.A. Stoltz, D.K. Meyerholz, M.J. Welsh, Origins of cystic fibrosis lung disease, N. Engl. J. Med. 372 (2015) 351–362.

[3] F. Ratjen, S.C. Bell, S.M. Rowe, C.H. Goss, A.L. Quittner, A. Bush, Cystic fibrosis, Nat. Rev. Dis. Primers 1 (2015), 15010.

[4] J.F. Hunt, C. Wang, R. C Ford, Cystic fibrosis transmembrane conductance regulator (ABCC7) structure, Cold Spring Harb. Perspect. Med. 3 (2013), a009514.

[5] H.A. Lewis, X. Zhao, C. Wang, J.M. Sauder, I. Rooney, B.W. Noland, D. Lorimer, M.C. Kearins, K. Conners, B. Condon, P.C. Maloney, W.B. Guggino, J.F. Hunt, S. Emtage, Impact of the F508 mutation in first nucleotide-binding domain of human cystic fibrosis transmembrane conductance regulator on domain folding and structure, J. Biol. Chem. 280 (2005) 1346–1353.

[6] S.J. Kim, W.R. Skach, Mechanisms of CFTR folding at the endoplasmic reticulum, Front. Pharmacol. 3 (2012), https://doi.org/10.3389/fphar.2012.00201, 1e11.

[7] T. Okiyoneda, G. Veit, J.F. Dekkers, M. Bagdany, N. Soya, H. Xu, A. Roldan, A.S. Verkman, M. Kurth, A. Simon, T. Hegedus, J.M. Beekman, G.L. Lukacs, Mechanism-based corrector combination restores DF508-CFTR folding and function, Nat. Chem. Biol. 9 (2013), 444e454, https://doi.org/10.1038/nchembio.1253.

[8] K. Du, M. Sharma, G.L. Lukacs, The F508 cystic fibrosis mutation impairs domain-domain interactions and arrests post-translational folding of CFTR, Nat. Struct. Mol. Biol. 12 (2005) 17–25.

[9] J.P. Mornon, P. Lehn, I. Callebaut, Atomic model of human cystic fibrosis transmembrane conductance regulator: membrane-spanning domains and coupling interfaces, Cell. Mol. Life Sci. 65 (2008) 2594–2612.

[10] A.W.R. Serohijos, T. Hegedus, A.A. Aleksandrov, L. He, L. Cui, N.V. Dokholyan, J.R. Riordan, Phenylalanine-508 mediates a cytoplasmic-membrane domain contact in the CFTR 3D structure crucial to assembly and channel function, Proc. Natl. Acad. Sci. U.S.A. 105 (2008) 3256–3261.

[11] P.H. Thibodeau, J.M. 3rd, Richardson, W. Wang, L. Millen, J. Watson, J.L. Mendoza, K. Du, S. Fischman, H. Senderowitz, G.L. Lukacs, K. Kirk, P.J. Thomas, The cystic fibrosis-causing mutation F508 affects multiple steps in cystic fibrosis transmembrane conductance regulator biogenesis, J. Biol. Chem. 285 (2010) 35825–35835.

[12] G.L. Lukacs, A.S. Verkman, CFTR: folding, misfolding and correcting the F508 conformational defect, Trends Mol. Med. 18 (2012) 81–91.

[13] C.M. Farinha, P. Matos, M.D. Amaral, Control of cystic fibrosis transmembrane conductance regulator membrane trafficking: not just from the endoplasmic reticulum to the Golgi, FEBS J. 280 (2013) 4396–4406.

[14] G.L. Lukacs, X.B. Chang, C. Bear, N. Kartner, A. Mohamed, J.R. Riordan, S. Grinstein, The F508 mutation decreases the stability of cystic fibrosis transmembrane conductance regulator in the plasma membrane: determination of functional half-lives on transfected cells, J. Biol. Chem. 268 (1993) 21592–21598.

[15] W. Dalemans, P. Barbry, G. Champigny, S. Jallat, K. Dott, D. Dreyer, R.G. Crystal, A. Pavirani, J.-P. Lecocq, M. Lazdunski, Altered chloride ion channel kinetics associated with the F508 cystic fibrosis mutation, Nature 354 (1991) 526–528.

[16] F. Van Goor, S. Hadida, P.D.J. Grootenhuis, B. Burton, J.H. Stack, K.S. Straley, C.J. Decker, M. Miller, J. McCartney, E.R. Olson, J.J. Wine, R.A. Frizzell, M. Ashlock, P.A. Negulescu, Correction of the F508del-CFTR protein processing defect in vitro by the investigational drug VX-809, Proc. Natl. Acad. Sci. U.S.A. 108 (2011) 18843–18848.

[17] F. Van Goor, S. Hadida, P.D.J. Grootenhuis, B. Burton, D. Cao, T. Neuberger, A. Turnbull, A. Singh, J. Joubran, A. Hazlewood, J. Zhou, J. McCartney, V. Arumugam, C. Decker, J. Yang, C. Young, E.R. Olson, J.J. Wine, R.A. Frizzell, M. Ashlock, P. Negulescu, Rescue of CF airway epithelial cell function in vitro by a CFTR potentiator, VX-770, Proc. Natl. Acad. Sci. U.S.A. 106 (2009) 18825–18830.

[18] J.P. Clancy, S.M. Rowe, F.J. Accurso, M.L. Aitken, R.S. Amin, M.A. Ashlock, M. Ballmann, M.P. Boyle, I. Bronsveld, P.W. Campbell, K. De Boeck, S.H. Donaldson, H.L. Dorkin, J.M. Dunitz, P.R. Durie, M. Jain, A. Leonard, K.S. McCoy, R.B. Moss, J.M. Pilewski, D.B. Rosenbluth, R.C. Rubenstein, M.S. Schechter, M. Botfield, C.L. Ordoñez, G.T. Spencer-Green, L. Vernillet, S. Wisseh, K. Yen, M.W. Konstan, Results of a phase IIa study of VX-809, an investigational CFTR corrector compound, in subjects with cystic fibrosis homozygous for the F508del-CFTR mutation, Thorax 67 (2012) 12–18.

[19] P. A Flume 1, T.G. Liou, D. S Borowitz, H. Li, K. Yen, C.L. Ordoñez, D.E. Geller, VX 08-770-104 Study Group Ivacaftor in subjects with cystic fibrosis who are homozygous for the F508del-CFTR mutation, Chest 142 (2012) 718–724.

[20] C.E. Wainwright, J.S. Elborn, B.W. Ramsey, G. Marigowda, X. Huang, M. Cipolli, C. Colombo, J.C. Davies, K. De Boeck, P.A. Flume, M.W. Konstan, S. A McColley, K. McCoy, E.F. McKone, A. Munck, F. Ratjen, S.M. Rowe, D. Waltz, M.P. Boyle, TRAFFIC Study Group, TRANSPORT Study Group Lumacaftor-ivacaftor in patients with cystic fibrosis homozygous for Phe508del CFTR, N. Engl. J. Med. 373 (2015) 220–231.

[21] S.H. Donaldson, J.M. Pilewski, M. Griese, J. Cooke, L. Viswanathan, E. Tullis,

J.C. Davies, J.A. Lekstrom-Himes, L.T. Wang, VX11-661-101 Study Group Tezacaftor/Ivacaftor in subjects with cystic fibrosis and F508del/F508del-CFTR or F508del/G551D-CFTR, Am. J. Respir. Crit. Care Med. 197 (2018) 214–224.
[22] H. Li, E. Pesce, D.N. Sheppard, A.K. Singh, N. Pedemonte, Therapeutic approaches to CFTR dysfunction: from discovery to drug development, J. Cyst. Fibros. 17 (2018) S14–S21, https://doi.org/10.1016/j.jcf.2017.08.013.
[23] F.H. Holguin, Triple CFTR modulator therapy for cystic fibrosis, N. Engl. J. Med. 379 (2018) 1671–1672, https://doi.org/10.1056/NEJMe1811996.
[24] D. Keating, G. Marigowda, L. Burr, C. Daines, M.A. Mall, E. F McKone, B.W. Ramsey, S.M. Rowe, L.A. Sass, E. Tullis, C.M. McKee, S.M. Moskowitz, S. Robertson, J. Savage, C. Simard, F. Van Goor, D. Waltz, F. Xuan, T. Young, J.L. Taylor-Cousar, VX16-445-001 Study Group VX-445-Tezacaftor-Ivacaftor in patients with cystic fibrosis and one or two Phe508del Alleles, N. Engl. J. Med. 379 (2018) 1612–1620.
[25] N. Liessi, E. Cichero, E. Pesce, M. Arkel, A. Salis, V. Tomati, M. Paccagnella, G. Damonte, B. Tasso, L.J.V. Galietta, N. Pedemonte, P. Fossa, E. Millo, Synthesis and biological evaluation of novel thiazole- VX-809 hybrid derivatives as F508del correctors by QSAR-based filtering tools, Eur. J. Med. Chem. 144 (2018) 179–200.
[26] C. Sinha, W. Zhang, C.S. Moon, M. Actis, S. Yarlagadda, K. Arora, K. Woodroofe, J.P. Clancy, S. Lin, A.G. Ziady, R. Frizzell, N. Fujii, A.P. Naren, Capturing the direct binding of CFTR correctors to CFTR using click chemistry, Chembiochem 16 (2015) 2017–2022.
[27] J.L. Taylor-Cousar, A. Munck, E.F. McKone, C.K. van der Ent, A. Moeller, C. Simard, L.T. Wang, E.P. Ingenito, C. McKee, Y. Lu, J. Lekstrom-Himes, J.S. Elborn, Tezacaftor -ivacaftor in patients with cystic fibrosis homozygous for Phe508del, N. Engl. J. Med. 377 (2017) 2013–2023.
[28] X. Wang, B. Liu, X. Searle, C. Yeung, A. Bogdan, S. Greszler, A. Singh, Y. Fan, A.M. Swensen, T. Vortherms, C. Balut, Y. Jia, K. Desino, W. Gao, H. Yong, C. Tse, P. Kym, Discovery of 4-[(2R,4R)-4-({[1-(2,2-Difluoro-1,3-benzodioxol-5-yl) cyclopropyl]carbonyl}amino)-7-(difluoromethoxy)-3,4-dihydro-2H-chromen-2-yl]benzoic acid (ABBV/GLPG-2222), a potent cystic fibrosis transmembrane conductance regulator (CFTR) corrector for the Treatment of Cystic Fibrosis, J. Med. Chem. 61 (2018) 1436–1449.
[29] P.R. Kym, X. Wang, X.B. Searle, B. Liu, M.C. Yeung, Preparation of Substituted Tetrahydropyrans as Cystic Fibrosis Transmembrane Conductance Regulator (CFTR) Modulators, 2016. US20160122331A1.
[30] C.M. Farinha, J. King-Underwood, M. Sousa, A.R. Correia, B.J. Henriques, M. Roxo-Rosa, A.C. Da Paula, J. Williams, S. Hirst, C.M. Gomes, M.D. Amaral, Revertants, low temperature, and correctors reveal the mechanism of F508del-CFTR rescue by VX-809 and suggest multiple agents for full correction, Chem. Biol. 20 (2013) 943–955.
[31] R.P. Hudson, J.E. Dawson, P.A. Chong, Z. Yang, L. Millen, P.J. Thomas, C.G. Brouillette, J.D. Forman-Kay, Direct binding of the corrector VX-809 to human CFTR NBD1: evidence of an allosteric coupling between the binding site and the NBD1:CL4 interface, Mol. Pharmacol. 92 (2017) 124–135.
[32] H.Y. Ren, D.E. Grove, O. De La Rosa, S.A. Houck, P. Sopha, F. Van Goor, B.J. Hoffman, D.M. Cyr, VX-809 corrects folding defects in cystic fibrosis transmembrane conductance regulator protein through action on membrane-spanning domain 1, Mol. Biol. Cell 19 (2013) 3016–3024.
[33] N. Odolczyk, J. Fritsch, C. Norez, N. Servel, M.F. da Cunha, S. Bitam, A. Kupniewska, L. Wiszniewski, J. Colas, K. Tarnowski, D. Tondelier, A. Roldan, E.L. Saussereau, P. Melin-Heschel, G. Wieczorek, G. L Lukacs, M. Dadlez, G. Faure, H. Herrmann, M. Ollero, F. Becq, P. Zielenkiewicz, A. Edelman, Discovery of novel potent ΔF508-CFTR correctors that target the nucleotide binding domain, EMBO Mol. Med. 5 (2013) 1484–1501.
[34] M. Rusnati, D. Sala, A. Orro, A. Bugatti, G. Trombetti, E. Cichero, C. Urbinati, M. Di Somma, E. Millo, L. Galietta, L. Milanesi, P. Fossa, P. D'Ursi, Speeding up the identification of cystic fibrosis transmembrane conductance regulator-targeted drugs: an approach based on bioinformatics strategies and surface plasmon resonance, Molecules 23 (2018), 120.
[35] Y. Wang, W. Cai, G. Zhang, T. Yang, Q. Liu, Y. Cheng, L. Zhou, Y. Ma, Z. Cheng, S. Lu, Y.-G. Zhao, W. Zhang, Z. Xiang, S. Wang, L. Yang, Q. Wu, L.A. Orband-Miller, Y. Xu, J. Zhang, R. Gao, M. Huxdorf, J.N. Xiang, Z. Zhong, J.D. Elliott, S. Leung, X. Lin, Discovery of novel N-(5-(arylcarbonyl)thiazol-2-yl)amides and N-(5-(arylcarbonyl)thiophen-2-yl)amides as potent RORγt inhibitors, Bioorg. Med. Chem. 22 (2) (2014) 692–702.
[36] Z. Abedi-Jazini, J. Safari, Z. Zarnegar, M. Sadeghi, A Simple and Efficient Method for the Synthesis of 2-Aminothiazoles under Mild Conditions Polycyclic Aromatic Compounds, vol. 38, 2018, pp. 1–5, 3.
[37] E. Bodio, K. Julienne, S.G. Gouin, A. Faivre-Chauvet, D. Deniaud, Efficient synthesis of new tetradentate ligands with potential applications for 64Cu PET-imaging, Bioorg. Med. Chem. Lett 21 (2011) 924–927.
[38] P. D'Ursi, M. Uggeri, C. Urbinati, E. Millo, G. Paiardi, L. Milanesi, R.C. Ford, J. Clews, X. Meng, P. Bergese, A. Ridolfi, N. Pedemonte, P. Fossa, A. Orro, M. Rusnati, Exploitation of a novel biosensor based on the full-length human F508de1-CFTR with computational studies, biochemical and biological assays for the characterization of a new Lumacaftor/Tezacaftor analogue, Sensor. Actuator. B Chem. 301 (2019), 127131.
[39] Cousins R.D., Elliott J.D., Lago M.A., Leber J.D., Peishoff C.E., Endothelin receptor antagonists US 2002/0002177 A1.
[40] E. Pesce, M. Bellotti, N. Liessi, S. Guariento, G. Damonte, E. Cichero, A. Galatini, A. Salis, A. Gianotti, N. Pedemonte, O. Zegarra-Moran, P. Fossa, L.J.V. Galietta, E. Millo, Synthesis and structure-activity relationship of aminoarylthiazole derivatives as correctors of the chloride transport defect in cystic fibrosis, Eur. J. Med. Chem. 99 (2015) 14–35.
[41] J.D. Hall, H. Wang, L.J. Byrnes, S. Shanker, K. Wang, I.V. Efremov, P.A. Chong, J.D. Forman-Kay, A.E. Aulabaugh, Binding screen for cystic fibrosis transmembrane conductance regulator correctors finds new chemical matter and yields insights into cystic fibrosis therapeutic strategy, Protein Sci. 25 (2016) 360–373.
[42] I. Reulecke, G. Lange, J. Albrecht, R. Klein, M. Rarey, Towards an integrated description of hydrogen bonding and dehydration: decreasing false positives in virtual screening with the HYDE scoring function, ChemMedChem 3 (2008) 885–897.
[43] N. Schneider, S. Hindle, G. Lange, R. Klein, J. Albrecht, H. Briem, K. Beyer, H. Claußen, M. Gastreich, C. Lemmen, M. Rarey, Substantial improvements in large-scale redocking and screening using the novel HYDE scoring function, J. Comput. Aided Mol. Des. 26 (2012) 701–723.
[44] L. O'Ryan, T. Rimington, N. Cant, R.C. Ford, Expression and purification of the cystic fibrosis transmembrane conductance regulator protein in Saccharomyces cerevisiae, JoVE 10 (2012), 61.
[45] N. Pollock, N. Cant, T. Rimington, R.C. Ford, Purification of the cystic fibrosis transmembrane conductance regulator protein expressed in Saccharomyces cerevisiae, JoVE 10 (2014), 87.
[46] H.H. Trutnau, New multi-step kinetics using common affinity biosensors saves time and sample at full access to kinetics and concentration, J. Biotechnol. 124 (2006) 191–195.